Supplemental Material can be found at:
http://www.jbc.org/cgi/content/full/M705621200/DC1

THE JOURNAL OF BIOLOGICAL CHEMISTRY VOL. 283, NO. 6, pp. 3594–3606, February 8, 2008

Heparan Sulfate Regulates Self-renewal and Pluripotency of Embryonic Stem Cells*[S]

Received for publication, July 9, 2007, and in revised form, October 10, 2007 Published, JBC Papers in Press, November 16, 2007, DOI 10.1074/jbc.M705621200

Norihiko Sasaki[‡§], Kazuhiko Okishio[‡], Kumiko Ui-Tei[¶], Kaoru Saigo[¶], Akiko Kinoshita-Toyoda[§‖], Hidenao Toyoda[§‖], Tomoaki Nishimura[‡‡], Yasuo Suda[§**‡‡], Michiko Hayasaka[§§], Kazunari Hanaoka[§§], Seiji Hitoshi[¶¶], Kazuhiro Ikenaka[¶¶], and Shoko Nishihara[‡§1]**

*From the [‡]Laboratory of Cell Biology, Department of Bioinformatics, Faculty of Engineering, Soka University, 1-236 Tangi-cho, Hachioji, Tokyo 192-8577, the [¶]Department of Biophysics and Biochemistry, Graduate School of Science, the University of Tokyo, 7-3-1 Hongo, Bunkyo-ku, Tokyo 113-0033, the [‖]Department of Bioanalytical Chemistry, Graduate School of Pharmaceutical Sciences, Chiba University, 1-33 Yayoi, Inage, Chiba 263-8522, the **Department of Nanostructure and Advanced Materials, Graduate School of Science and Engineering, Kagoshima University, 1-21-40 Kohrimoto, Kagoshima 890-0065, [‡‡]Sudx-Biotec Corporation, KIBC 461, 5-5-2, Minatojima-minami, Chuo-ku, Kobe 650-0047, [§§]Laboratory of Molecular Embryology, Department of Bioscience, Kitasato University School of Science, 1-15-1 Kitasato, Sagamihara, Kanagawa 228, [¶¶]Division of Neurobiology and Bioinformatics, National Institute for Physiological Sciences, 38 Nishigonaka Myodaiji, Okazaki, Aichi 444-8585, and [§]Core Research for Evolutional Science and Technology of Japan Science and Technology Agency, Kawaguchi Center Building, 4-1-8, Hon-cho, Kawaguchi, Saitama 332-0012, Japan*

Embryonic stem (ES) cell self-renewal and pluripotency are maintained by several signaling cascades and by expression of intrinsic factors, such as Oct3/4 and Nanog. The signaling cascades are activated by extrinsic factors, such as leukemia inhibitory factor, bone morphogenic protein, and Wnt. However, the mechanism that regulates extrinsic signaling in ES cells is unknown. Heparan sulfate (HS) chains are ubiquitously present as the cell surface proteoglycans and are known to play crucial roles in regulating several signaling pathways. Here we investigated whether HS chains on ES cells are involved in regulating signaling pathways that are important for the maintenance of ES cells. RNA interference-mediated knockdown of HS chain elongation inhibited mouse ES cell self-renewal and induced spontaneous differentiation of the cells into extraembryonic endoderm. Furthermore, autocrine/paracrine Wnt/β-catenin signaling through HS chains was found to be required for the regulation of Nanog expression. We propose that HS chains are important for the extrinsic signaling required for mouse ES cell self-renewal and pluripotency.

Embryonic stem (ES)[2] cells from the inner cell mass of preimplantation mouse embryos can be used to establish pluripotent cell lines (1, 2). ES cells retain the ability to differentiate into the representative cell types of all three germ layers of the developing mouse embryo. Human ES cell lines have been derived (3), and the pluripotency of these cells is a feature providing considerable potential for exploitation in the development of cell replacement therapies to treat human disease. However, the molecular mechanisms that control pluripotency and differentiation of ES cells are largely unknown. It will be essential to gain a better understanding of these mechanisms to exploit the potential of ES cells for therapeutic purposes.

A number of studies have investigated the factors controlling pluripotency of mouse ES (mES) cells (4). Self-renewal of mES cells is sustained by signals mediated by the cytokine, leukemia inhibitory factor (LIF) (5, 6). LIF signals through the heteromeric receptor gp130 and the low affinity LIF receptor to induce activation of STAT3 (7–10). However, exposure of cells to serum is also required for LIF-mediated maintenance of self-renewal (11).

Treatment of mES cells with the bone morphogenic proteins (BMPs) BMP2 and BMP4 or with growth differentiation factor 6 can substitute for serum. The ability of BMP/growth differentiation factor 6 to promote self-renewal requires co-stimulation with LIF (11). BMP induces the expression of inhibitor of differentiation (*Id*) genes through activation of Smad signaling, and the *Id* gene products suppress expression of genes involved in the induction of neural differentiation (11). Thus, BMP suppresses neural differentiation and, in combination with LIF, is sufficient to sustain self-renewal of mES cells without the need for feeder cells or serum factors.

Wnt signaling was shown to play a role in the regulation of self-renewal of both mouse and human ES cells independently

* This work was supported by Core Research for Evolutional Science and Technology of Japan Science and Technology Agency and The Ministry of Education, Culture, Sports, Science, and Technology Haiteku (2004–2008). The costs of publication of this article were defrayed in part by the payment of page charges. This article must therefore be hereby marked "*advertisement*" in accordance with 18 U.S.C. Section 1734 solely to indicate this fact.

[S] The on-line version of this article (available at http://www.jbc.org) contains supplemental data 1–6.

[1] To whom correspondence should be addressed: Laboratory of Cell Biology, Dept. of Bioinformatics, Faculty of Engineering, Soka University, 1-236 Tangi-cho, Hachioji, Tokyo 192-8577, Japan. Tel.: 81-426-91-8140; Fax: 81-426-91-9315; E-mail: shoko@t.soka.ac.jp.

[2] The abbreviations used are: ES, embryonic stem; HS, heparan sulfate; mES, mouse ES; LIF, leukemia inhibitory factor; BMP, bone morphogenic protein; Id, inhibitor of differentiation; FGF, fibroblast growth factor; siRNA, small interfering RNA; MEF, mouse embryonic fibroblast; EB, embryoid body; BIO, 6-bromoindirubin-3′-oxine; MeBIO, 1-methyl-6-bromoindirubin-3′-oxine; CS, chondroitin sulfate; BSA, bovine serum albumin; HPLC, high performance liquid chromatography; AP, alkaline phosphatase; Tcf, T-cell-specific factor; SPR, surface plasmon resonance; vWF, von Willebrand factor; RNAi, RNA interference; PI3K, phosphoinositide 3-kinase; ERK, extracellular signal-regulated kinase; FBS, fetal bovine serum; FACS, fluorescence-activated cell sorter; IL, interleukin; RT, reverse transcription; EGFP, enhanced green fluorescent protein; ERK, extracellular signal-regulated kinase.

of LIF/STAT3 signaling (12). Wnt proteins play roles in the regulation of gene expression, cell proliferation, and differentiation and in the maintenance of cell polarity (13). The binding of Wnt protein to its cognate receptor, Frizzled, results in the inhibition of glycogen synthase kinase-3. This in turn leads to the stabilization and nuclear accumulation of β-catenin and to changes in gene transcription. Signaling by this canonical Wnt pathway has been suggested to result in downstream activation of expression of the homeoprotein Nanog, a transcription factor that is essential for maintenance of the inner cell mass and of ES cell pluripotency (14, 15). The activation of Nanog sustains ES cell self-renewal without the use of feeder cells or treatment with LIF (12).

Heparan sulfate (HS) proteoglycans are ubiquitously present in the extracellular matrix and on the cell surface. The HS polysaccharide chains of the proteoglycans are covalently attached to several core proteins (16). HS chains are synthesized in the Golgi apparatus by several enzymes, including members of the EXT protein family. The chains consist of repeating disaccharide units of D-glucuronic acid-*N*-acetyl-D-glucosamine that are modified differentially by epimerization and sulfation (16). A large number of physiologically important molecules can bind to specific sulfated regions of HS chains (17). Genetic studies have shown that HS chains regulate biological functions by interacting with various extracellular signaling molecules, such as members of the fibroblast growth factor (FGF) family, Wnt/Wingless (Wg), Hedgehog (Hh), and BMP (18). In *Drosophila,* for example, analyses of mutations of the *EXT* family genes *tout-velu* (*ttv*), *sister of ttv* (*sotv*), and *brother of ttv* (*botv*) have indicated that HS chains are required for signaling and distribution of Hh, Wg, and Decapentaplegic (the functional ortholog of mammalian BMP2 and BMP4) during embryogenesis and wing development (19–22). In mammals, the importance of HS chains in development has been demonstrated by analyses of mutations of enzymes required for HS chain modification, and FGF and Indian hedgehog signaling through HS chains has been suggested to be required during development (18, 23–26). Thus, there is evidence that HS chains have essential functions in development, however, it is not yet clear what role HS chains play in the regulation of early embryogenesis and in ES cells.

Our current understanding suggests that HS chains may contribute to the maintenance of ES cell self-renewal by regulating the activities of several signaling pathways, such as LIF/STAT3, BMP/Smad, and Wnt/β-catenin. In the present study, we investigated the contribution of HS chains to the regulation of ES cell self-renewal and pluripotency. We used small interfering RNA (siRNA) to knockdown *EXT1*, which is required for HS chain elongation. Transfected mES cells grew more slowly than untreated control cells and differentiated into extraembryonic endoderm even in the presence of LIF and serum. This is the first demonstration of the importance of HS chains for the maintenance of self-renewal and pluripotency of mES cells.

EXPERIMENTAL PROCEDURES

Cell Culture and Transfection—R1 (27) and E14TG2a (28) mES cell lines were maintained on mouse embryonic fibroblasts (MEFs) inactivated with 10 μg/ml mitomycin C (Sigma) in ES medium (Dulbecco's modified Eagle's medium supplemented with 15% FBS {Hyclone}, 1% penicillin/streptomycin {Invitrogen}, 0.1 mM mercaptoethanol {Invitrogen}, and 0.1 mM nonessential amino acids {Invitrogen}) with 1000 units/ml LIF (Chemicon). We generated siRNA expression plasmids targeting *EXT1* and *EGFP* as negative control by inserting of the corresponding double strand DNAs into the BamHI-HindIII site of pSilencer 3.1-H1 (Ambion). The sequences used for RNAi were designed as described previously (29): *EGFP*, 5′-GATCCCGCCACAACGTCTATATCATGGGGAAAATCCATGATATAGACGTTGTGGCTTTTTTGGAAA-3′; *EXT1-1*, 5′-GATCCCGTCCTACCGCAGTATTCATCTGCTTCCTGTCACAGATGAATACTGCGGTAGGACTTTTTTGGA-3′; *EXT1-2*, 5′-GATCCCGGTCTATTCATCAGGATAAAAGCTTCCTGTCACTTTTATCCTGATGAATAGACCTTTTTTA-3′. For transient knockdown of *EXT1* mRNA by RNAi, siRNA expression plasmids for *EXT1* were transfected into mES cells as follows. Prior to transfection, the mES cells were harvested, replated at 1×10^6 cells on gelatin-coated feeder-free 60 mm tissue culture dishes (Iwaki) in ES medium with LIF, and incubated for 16 h. On day 1, the cells were transfected with an siRNA expression plasmid (2 μg per culture dish) using Lipofectamine 2000 (Invitrogen). On day 2, the cells were harvested and replated at 3×10^6 cells on gelatin-coated feeder-free 60 mm tissue culture dishes in ES medium with LIF and 2 μg/ml puromycin (Sigma). In general, puromycin selection of transfected cells was carried out for 24 h. On day 3 (2 days after transfection), the cells were harvested and analyzed as described below.

For differentiation into embryoid bodies (EBs), the cells were transferred on day 3 to low-cell-binding 60 mm dishes (Nunc) and cultured in ES medium without LIF. The numbers of small noncystic EBs and large EBs filled with cystic cavity were counted by microscopic examination. EBs were fixed overnight in 4% paraformaldehyde at 4 °C, dehydrated, embedded in paraffin and sectioned at 10 μm. Sections were stained with hematoxylin and eosin (Merck).

For morphological observation and real time PCR analysis of differentiation markers, the cells were replated on day 2 and incubated with puromycin for 3 days.

For exogenous activation of Wnt/β-catenin signaling, the cells were treated with 2 μM 6-bromoindirubin-3′-oxine (BIO; R&D Systems), a specific pharmacological inhibitor of glycogen synthase kinase-3 or 1-methyl-6-bromoindirubin-3′-oxine (MeBIO; R & D Systems), an inactive analog of BIO during transfection and culture.

FACS Analysis—Two days after transfection, mES cells were harvested and the cell suspension was incubated with mouse IgM negative isotype control (Chemicon), anti-HS antibody 10E4 (Seikagaku Corp.) or anti-chondroitin sulfate (CS) antibody 2H6 (Seikagaku Corp.) diluted in FACS buffer (0.5% bovine serum albumin (BSA) and 0.1% sodium azide in PBS). After washing, the cell suspension was incubated with fluorescein isothiocyanate-conjugated secondary antibody (Sigma) diluted in FACS buffer. Cell sorting and analysis were performed using a FACSAria Cell Sorter (BD Biosciences).

High Performance Liquid Chromatography (HPLC) Analysis of Unsaturated Disaccharides—Two days after transfection, mES cells were harvested and fluorometric post-column HPLC analysis of unsaturated disaccharides from HS chains was performed as reported previously (30).

Molecular Size Analysis of HS Chains—One day after transfection, mES cells were harvested, replated at 1.5×10^6 cells per well in 6-well 0.2% gelatin-coated plates and incubated in sulfate-free ES medium with LIF, puromycin and 100 μCi/ml $Na_2{}^{35}SO_4$ (ARC). After labeling for 24 h, the cells were washed twice with PBS and then treated with 1 mg/ml trypsin (WAKO) for 10 min at 37 °C. The trypsin was neutralized with 2 mg/ml trypsin inhibitor (Roche Applied Science). After centrifugation, the supernatants were treated with 0.5 M NaOH at 4 °C overnight and neutralized with 1 M acetic acid. The labeled galactosaminoglycans were eliminated by chondroitinase ABC (Seikagaku Corp.) digestion, desalted in a PD-10 column (GE Healthcare) and resistant HS chains were isolated by anion exchange chromatography on HiTrap DEAE FF (GE Healthcare) using sodium phosphate buffer (pH 6.0) containing 1.0 M NaCl as the eluent. The sizes of the purified HS chains were analyzed by gel chromatography on a Sephacryl S-300 column (GE Healthcare) (1 × 44 cm) and eluted with 50 mM Tris-HCl, pH 7.4, containing 0.2 M NaCl. Fractions (1 ml/fraction) were collected and analyzed for radioactivity using a scintillation counter. The purity of the labeled HS was determined by sensitivity to enzyme digestion with 5 milliunits of heparitinase I and II (Seikagaku Corp.) and heparinase (Seikagaku Corp.). Estimations of molecular mass values were derived from fractionation of several Dextran molecular size markers (Sigma) by gel chromatography and staining with orsinol solution.

Proliferation Assay—Two days after transfection, mES cells were harvested and replated in triplicate at 0.8×10^4 cells per well in 96-well 0.2% gelatin-coated plates in ES medium with LIF. Cell counting kit-8 (Dojindo) was added after 0 h, 24 h or 48 h and incubated further for 2 h. The soluble formazan product was measured at 450 nm.

Self-renewal Assay—Two days after transfection, mES cells were harvested and replated at 1×10^4 cells per gelatin coated 60 mm tissue culture dish in ES medium with LIF. For detection of undifferentiated cells, cells were fixed and stained with 5-bromo-4-chloro-3-indolyl phosphate-nitro blue tetrazolium (Nacalai Tesque) 5 days after replating. Alkaline phosphatase (AP) positive colonies were counted by microscopic examination. Colonies of tightly packed and flattened AP-positive cells were counted as undifferentiated, and colonies of mixtures of unstained and stained cells and entirely unstained cells with flattened irregular morphology were considered differentiated.

Immunoblotting—Two days after transfection, the culture solution for the mES cells was replaced with serum-free ES medium without LIF for 4 h and the cells were stimulated for 20 min with one of the following: 15% FBS, 1000 units/ml LIF, 10 ng/ml BMP4 (R&D Systems), 40 ng/ml basic FGF (Upstate Biotechnology) or 15% FBS plus 1000 units/ml LIF. For depletion of HS chains, mES cells were incubated with 5 milliunits of heparitinase I and II and heparinase for 2 h before extrinsic stimulation. Cells were lysed with lysis buffer (50 mM Tris-HCl, pH 7.4, 150 mM NaCl, 1% Triton X-100, 1 mM Na_3VO_4, 10 mM NaF, protease inhibitors).

To isolate nuclear extracts, cells were first suspended in 100 μl of buffer (10 mM Hepes, pH 7.4, 2 mM $MgCl_2$, 1 mM EDTA, 10 mM KCl, 1 mM dithiothreitol, protease inhibitors). After incubation for 15 min on ice, 12.5 μl of 5% Nonidet P-40 was added, the suspension was vortexed for 10 s, and incubated for a further 5 min on ice. The suspension was centrifuged at 13,000 rpm for 30 s. The supernatant was removed and the pellets, comprising the nuclear extracts, were washed with PBS and lysed with lysis buffer (25 mM Hepes, pH 7.4, 500 mM NaCl, 1 mM dithiothreitol, 10% glycerol, 0.2% Nonidet P-40, 5 mM $MgCl_2$). The purity of the cell fractionation (cytosol and nucleus) was confirmed in Western blot analysis using an anti-Yes monoclonal antibody (BD Biosciences) and an anti-Lamin B_1 antibody (Zymed Laboratories Inc.); these antibodies are specific for the cytosol and nucleus, respectively. Only low levels of cross-contamination were observed (<1%).

Ten micrograms of cell lysates or nuclear extracts were separated by 10% SDS-PAGE and transferred onto polyvinylidene difluoride membranes (Millipore). After blocking, the membranes were incubated with antibodies to STAT3 (BD Biosciences), phosphorylated STAT3 (Tyr-705 BD Biosciences), ERK-1/2 (Cell Signaling Technology), phosphorylated ERK-1/2 (Thr-183 and Thr-185; Sigma), Akt (BD Biosciences), phosphorylated Akt (Ser-472 and Ser-473; BD Biosciences), phosphorylated Smad1 (Ser-463 and Ser-465; Cell Signaling Technology), Yes (Santa Cruz Biotechnology), phosphorylated Src family (Tyr-416; Cell Signaling Technology), β-actin (Sigma), β-catenin (Cell Signaling Technology), phosphorylated β-catenin (Ser-33/37/Thr41; Cell Signaling Technology), Lamin B_1, Oct3/4 (Santa Cruz Biotechnology), or Nanog (ReproCELL). The membranes were then incubated with the appropriate peroxidase-conjugated secondary antibody (Cell Signaling Technology). After washing, the membranes were developed with ECL Plus reagents (GE Healthcare). For detection of phosphorylated Yes, cells were lysed with lysis buffer (30 mM Tris-HCl, pH 7.4, 150 mM NaCl, 1% Triton X-100, 0.5% sodium deoxycholate, 0.1% SDS, 10 mM EDTA, 1 mM Na_3VO_4, 10 mM NaF, protease inhibitors) and immunoprecipitated with 1 μg of anti-Yes monoclonal antibody and protein G Magnetic Beads (New England Biolabs); this approach was adopted as this is the only commercially available anti-phosphorylated Src family antibody that cross-reacts with phosphorylated Yes.

Luciferase Reporter Assay and Immunostaining—Transactivation of β-catenin on T-cell-specific factor (Tcf) was determined with a luciferase reporter assay. siRNA expression plasmid (2 μg) was cotransfected with reporter plasmid such as, TOPFLASH (2 μg, containing three Tcf binding sites, Upstate Biotechnology) or FOPFLASH (2 μg, containing inactive Tcf binding sites, Upstate Biotechnology) and pCH110 (0.2 μg, containing β-galactosidase, GE Healthcare) as control of transfection efficiency using Lipofectamine 2000 as described above. Cell lysates were prepared 3 days after transfection and luciferase activity was measured with Dual-Light® System (Applied Biosystems). Luminescence was measured with a Lumat LB9501 luminometer (Berthold). Luciferase activity was normalized for transfection efficiency by β-galactosidase activity.

Relative luciferase activity is defined as the ratio of luciferase activity of TOPFLASH to that of FOPFLASH.

For immunostaining of β-catenin, mES cells were fixed with 4% paraformaldehyde and permeabilized with 0.1% saponin 3 days after transfection. After washing and subsequent blocking, cells were stained with an anti-β-catenin antibody. After washing, cells were stained with fluorescein isothiocyanate-conjugated secondary antibody (Chemicon) and counterstained with propidium iodide (BD Biosciences). Immunofluorescence images were taken using an LSM5Pascal confocal laser scanning microscope (Carl Zeiss) with ×40/1.3 objectives at room temperature.

^{125}I-Labeled Wnt3a Binding Assay—Two micrograms of recombinant mouse Wnt3a (R&D Systems) were iodinated with 100 μCi of ^{125}I-sodium (ARC) using iodogen-precoated reaction tubes (Pierce) according to manufacturer's instructions. Radiolabeled Wnt3a was separated from unincorporated ^{125}I-sodium on a PD-10 column. The specific activity of the radiolabeled Wnt3a was 1.85×10^4 cpm/ng protein. For the binding assay, mES cells were harvested 2 days after transfection and replated in triplicate at 5×10^5 cells per well in 24-well 0.2% gelatin-coated plates. The cells were allowed to attach for 3 h and then washed three times with ice-cold binding buffer (serum-free ES medium containing 1 mg/ml BSA and 0.1% sodium azide). After incubating with 80 ng/ml ^{125}I-labeled Wnt3a either alone or in the presence of 100 μg/ml heparin (Sigma) in binding buffer for 3 h at 4 °C, the cells were gently washed three times with ice-cold binding buffer and lysed with 0.2 N NaOH. The amount of radiolabeling in each extract was counted with a gamma counter (Aloka).

Surface Plasmon Resonance (SPR) Analysis—Heparin (Nacalai Tesque) was dialyzed against distilled water using an MWCO3500 membrane (SpectroPore) and lyophilized. Then the heparin was conjugated with a monovalent linker molecule to prepare the ligand conjugate for the immobilization of heparin on the gold-coated chip as previously described (31). The surface of the gold-coated chip (SUDx-Biotec) was oxidatively washed with UV ozone cleaner (Structure Probe Inc.) for 20 min. The chips were then immersed in 1 μM of the ligand-conjugate in 50% (v/v) methanol solution overnight at room temperature with gentle agitation to prepare Sugar Chips with immobilized heparin. The Sugar Chips were washed sequentially with water, PBS containing 0.05% Tween 20 and water, and dried at room temperature.

The Sugar Chip with immobilized heparin was set on a prism with refraction oil (n_D = 1.518, Cargill Laboratories Inc.) in an SPR apparatus (SPR670M, Moritex). The SPR measurements were performed at room temperature in accordance with the manufacturer's instructions and using Tris-buffered saline (20 mM Tris-HCl, 150 mM NaCl, pH 7.4) containing 0.05% Tween 20 and 0.1% BSA as the running buffer at a flow rate of 15 μl/min. The kinetic binding parameters were calculated using the software of the manufacturer. We performed binding of BSA or von Willebrand factor (vWF) A1 to heparin, as negative and positive controls, respectively (supplemental data 1) (apparent association and dissociation rate constants k_a (M^{-1} s^{-1}) and k_d (s^{-1}) of vWF A1, 3.51×10^3, 4.38×10^{-3}, respectively; apparent equilibrium constant K_D (nM) for binding of vWF A1 to heparin, 1248.1).

RT-PCR and Real Time PCR—Total RNA was isolated from mES cells by TRIzol Reagent (Invitrogen) and subsequently reverse transcribed using an oligo-dT primer (Invitrogen) and a SuperscriptII first strand synthesis kit (Invitrogen). Primer sets for PCR amplification are listed in supplemental data 2. All cDNAs were amplified in quantitative ranges, which were confirmed by examining various cycles for the samples giving maximum levels of signals in each primer sets. Primers sets and probes for real time PCR are listed in supplemental data 3. Real time PCR was performed using an ABI PRISM® 7700 sequence detection system (Applied Biosystems). The relative amounts of each mRNA were normalized by *β-actin* mRNA in the same cDNA.

RESULTS

HS Chains Are Reduced by Knockdown of EXT1 mRNA—Hereditary multiple exostosis is an autosomal dominant disorder characterized by the development of benign cartilage-capped tumors at the juxta-epiphyseal regions of long bones (32). It is associated with mutation of either *EXT1* or *EXT2*, which encode glycosyltransferases possessing both D-glucuronic acid and GlcNAc-transferase activities that are necessary for HS chain elongation (33, 34). In the Golgi apparatus, EXT1 and EXT2 form a hetero-oligomeric complex that exhibits higher glycosyltransferase activity than either enzyme alone (35, 36). To examine the effect of reduced HS chain levels in ES cells, we knocked down expression of *EXT1* mRNA using RNAi. We designed two constructs expressing different siRNAs targeting *EXT1* (*EXT1-1* and *EXT1-2*), as described previously (29), and siRNAs targeting *EGFP* as a negative control. We represent mES cells transfected with *EGFP* siRNA expression plasmids as "control cells" throughout this paper. Real time PCR analysis performed 2 days after transfection of the cells with *EXT1* siRNA expression plasmids showed that the level of *EXT1* mRNA was reduced to about 20% that of control cells. In contrast, the expression of other nontargeted genes was unaffected by this treatment in the two mES lines tested (R1 and E14TG2a) (Fig. 1*A*). The knockdown effect on *EXT1* was maintained for at least 3 days following puromycin selection. We used E14TG2a to confirm the same knockdown effect on mES cells using one siRNA expression plasmid (*EXT1-1*) throughout all experiments.

Two days after transfection, we performed FACS analysis using an anti-HS antibody to determine whether HS chain expression was reduced by knockdown of *EXT1* mRNA. As shown in Fig. 1*B*, HS chains were abundant in mES cells, whereas CS chains were not. We observed a significant reduction in HS chain expression on the cell surface of cells transfected with an *EXT1* siRNA expression plasmid compared with control cells (Fig. 1*B*). The knockdown effect was higher using *EXT1-1* siRNA compared with *EXT1-2* siRNA. Reduction of HS chain expression was accompanied by a subtle increase in CS chain synthesis that correlated with the level of reduction of HS chains. Such an increase in CS chain expression was previously observed in *EXT1*-deficient ES cells derived from *EXT1* knock-out mice (25). The reduction of HS chain expression in

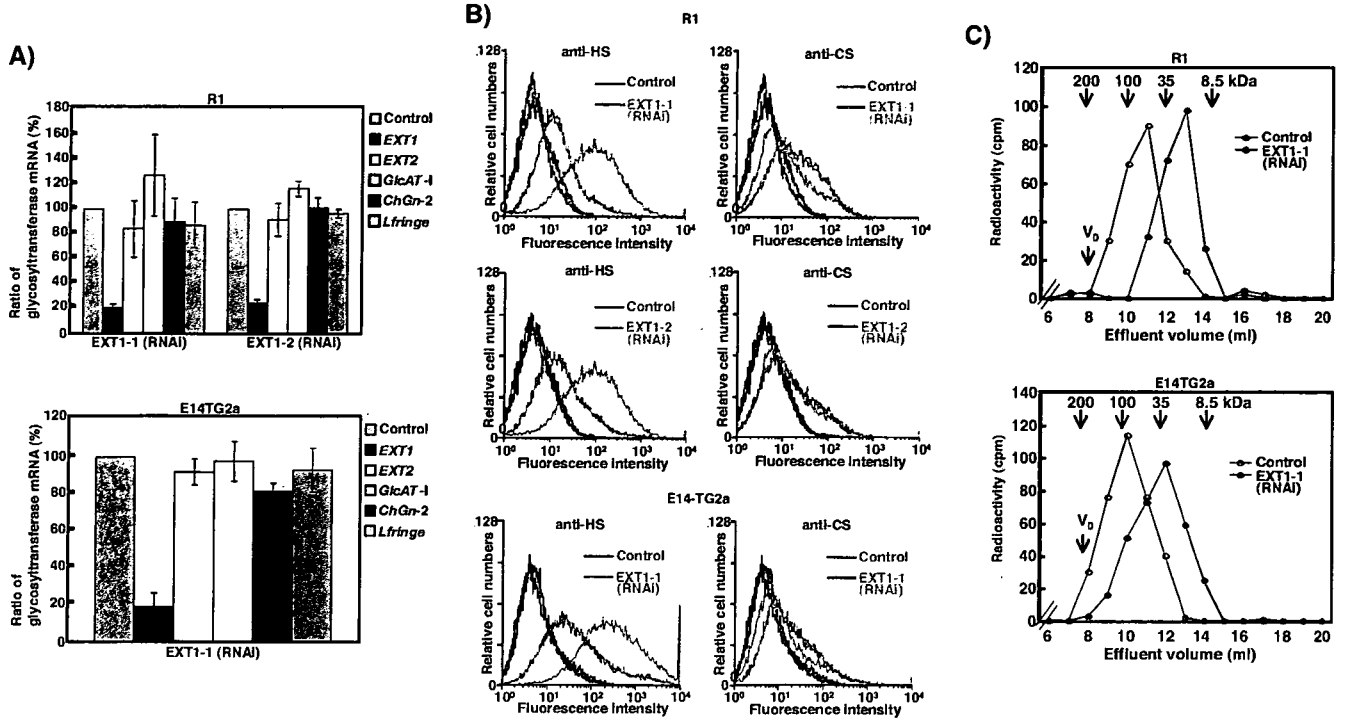

FIGURE 1. ***EXT1* siRNA induces efficient knockdown of *EXT1* mRNA and reduction of HS chains in mES cells.** *A*, real time PCR analysis of cells 2 days after transfection. The results are shown as the proportion (%) of expression of each glycosyltransferase mRNA relative to that observed in control cells: *GlcAT*, glucuronosyltransferase; *ChGn*, chondroitin β1,4-*N*-acetylgalactosaminyltransferase; *Lfringe*, lunatic fringe. The values shown are the means ± S.D. of three independent experiments. We used two constructs expressing different siRNAs targeting *EXT1* (*EXT1-1* and *EXT1-2*). *B*, FACS analysis of cells 2 days after transfection using an anti-HS antibody or anti-CS antibody (*black* and *blue lines* represent IgM isotype control of control and *EXT1*-deficient cells, respectively). Three independent experiments were performed and representative results are shown. *C*, molecular size analysis of HS chains from mES cell surface by gel chromatography on a Sephacryl S-300 column. The *open squares* and *closed squares* indicate the elution profiles of HS chains from control and *EXT1*-deficient cells, respectively. *Arrows* indicate the elution positions of dextran molecular mass standards.

EXT1-deficient cells was also confirmed by HPLC analysis of unsaturated disaccharides from HS chains (data not shown). We also examined the molecular sizes of HS chains derived from *EXT1*-deficient cell surface by gel chromatography. As is shown in Fig. 1*C*, the lengths of HS chains in *EXT1*-deficient cells (~35kDa) appeared to be reduced compared with control cells (50–150 kDa).

HS Chains Are Important for Self-renewal and Proliferation of mES Cells—We performed colony assays on *EXT1*-deficient cells to determine whether the resulting reduction in HS chain expression affected the frequency with which the cells remain in an undifferentiated state. The number of colonies derived from *EXT1*-deficient cells that remained in an undifferentiated state fell to about 50% that of control cells, even in the presence of LIF and serum (Fig. 2*A*). We next examined proliferation of transfected mES cells. As shown in Fig. 2*B*, the rate of proliferation of *EXT1*-deficient cells decreased significantly compared with control cells. These results suggest that the reduction in HS chain expression inhibited the capacity for both self-renewal and proliferation of mES cells, presumably because of reduced levels of HS chain-dependent signaling.

The Reduction of HS Chain Expression Increases Spontaneous Differentiation of mES Cells into Extraembryonic Endoderm—We compared the morphologies of control and *EXT1*-deficient cells. Four days after transfection in the presence of LIF, control cells appeared to be undifferentiated cells with modest packed morphology in which the cells preferentially adhered to one another, but differentiated cells with a flattened morphology also existed at low levels because of the feeder-free culture conditions (Fig. 3*A*). In contrast, almost all of the *EXT1*-deficient cells exhibited a flattened, differentiated morphology that, in some cells, was reminiscent of the stellate morphology of the parietal endoderm (37) (Fig. 3*A*). Furthermore, expression of *Oct3/4* and *Nanog*, which are markers of the undifferentiated state, was significantly decreased in *EXT1*-deficient cells compared with control cells (Fig. 3*B*), indicating that spontaneous differentiation of *EXT1*-deficient cells occurred more frequently than of control cells. Upon withdrawal of LIF, control cells exhibited a variety of flattened and differentiated morphologies (data not shown), suggesting that pluripotency had been maintained. However, most of the *EXT1*-deficient cells exhibited a parietal endoderm-like morphology (data not shown), as was the case in the presence of LIF.

To further characterize the transfected mES cells, we evaluated expression of several germ layer markers by real time PCR analysis of cells 4 days after transfection (Fig. 3, *B–D*). In the presence of LIF, we detected higher expression in *EXT1*-deficient cells of markers of the extraembryonic endoderm lineage (primitive endoderm, *Gata4* and *Gata6*; parietal endoderm, *Dab2* and *LamininB1*; and visceral endoderm, *Bmp2* and *Ihh*) than control cells (Fig. 3*C*), whereas other lineage markers (such as the trophoblast marker, *Cdx2*; the primitive ectoderm marker, *Fgf-5*; the neuroectoderm marker, *Isl1*; and the mesoderm marker, *Brachyury*) were weakly expressed (Fig. 3*D*).

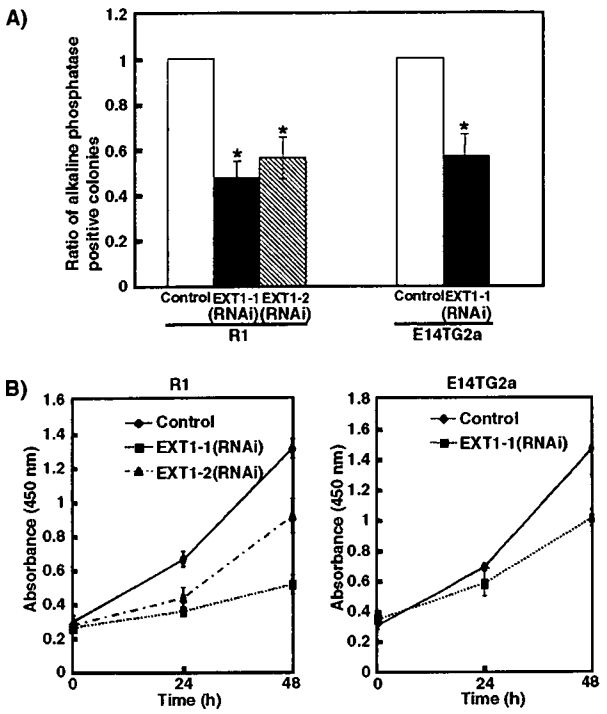

FIGURE 2. ***EXT1*-deficient cells show decreased potential for self-renewal and proliferation.** *A*, self-renewal assay. The ratio of AP-positive colonies is shown after normalization against control cells (value = 1). Approximately 70% of the colonies derived from the control cells remained in an undifferentiated state in feeder-free culture. The values shown are the means ± S.D. from three independent experiments, and significant values are indicated; *, $p < 0.01$, in comparison with control. *B*, proliferation assay. The values shown are the means ± S.D. from three independent experiments.

These results reflect the morphologies of *EXT1*-deficient cells as shown in Fig. 3*A*. Following withdrawal of LIF, *EXT1*-deficient cells underwent further differentiation. We observed only induction of extraembryonic endoderm lineage markers in these cultures compared with control cells (Fig. 3, *C* and *D*). Upon induction of differentiation of control cells, various markers of differentiation, including *Cdx2*, *Fgf-5*, and *Brachyury*, and extraembryonic endoderm lineage markers exhibited a further increase in expression associated with a decrease of expression of *Oct3/4* and *Nanog*, indicating that pluripotency had been maintained. Our analyses indicate that HS chains are important for the maintenance of the undifferentiated state and of pluripotency of mES cells and that signaling pathways mediated by HS chains may be involved in signaling pathways that control the differentiation of mES cells into the extraembryonic endoderm lineage.

We next examined the formation of EBs in suspension culture in control and *EXT1*-deficient cells. EB formation occurs during the *in vitro* differentiation of ES cells into the three germ layers, mesoderm, ectoderm, and endoderm. This differentiation process resembles the formation of the developing conceptus at the egg-cylinder stage. As shown in Fig. 3, *E* and *F*, almost all control cells formed large fluid-filled cystic EBs 6 days after EB formation, in which differentiation into the three germ layers had begun to proceed. In contrast, 53.02 ± 5.83% of *EXT1*-deficient cells formed noncystic and significantly small EBs. This suggests that the reduction in HS chain expression inhibited differentiation of *EXT1*-deficient cells into the three germ layers, supporting the results that differentiation of *EXT1*-deficient cells into nonextraembryonic endoderm lineage was inhibited in normal culture (Fig. 3, *D* and *E*). Similar results were obtained in cells transfected with the second siRNA expression plasmid targeting *EXT1* (*EXT1-2*) and also in a second mES cell line (E14TG2a; data not shown).

The Reduction of HS Chains Down-regulates Specific Signaling—Several signaling molecules have been shown to be important for the maintenance of mES cell self-renewal, for example, LIF/STAT3, BMP/Smad, Wnt/β-catenin, phosphoinositide 3-kinase (PI3K)/Akt, and members of the Src family (7–12, 38, 39). Therefore, we performed Western blot analysis of cell lysates prepared 2 days after transfection of control and *EXT1*-deficient cells to determine whether the activity of signaling molecules was affected by the reduction of HS chain expression. We observed a similar increase in the level of phosphorylation of Akt and Smad1 in control and *EXT1*-deficient cells following exposure to 15% FBS (supplemental data 4), suggesting that the serum-responsive signaling by PI3K and Smad was not affected by the reduced expression of HS chains. Moreover, we found that treatment of control or *EXT1*-deficient cells with LIF or BMP4 gave rise to similar increases in the phosphorylation of STAT3 and Smad1, respectively (Fig. 4, *A* and *B*). Heparitinase treatment was performed to examine the effect of HS chain depletion on BMP/Smad and LIF/STAT3 signaling. This treatment led to a reduction in BMP/Smad signaling but not of LIF/STAT3 signaling (Fig. 4, *C* and *D*), demonstrating that HS chains contribute to BMP signaling but not LIF signaling in mES cells. The level of phosphorylation of ERK in response to basic FGF treatment was reduced in *EXT1*-deficient cells compared with the level observed in control cells, suggesting that FGF signaling was reduced in *EXT1*-deficient cells (Fig. 4*B*) and more reduction was detected after heparitinase treatment (Fig. 4, *C* and *D*). Phosphorylation of the Src family member, cYes, which has been implicated in the maintenance of self-renewal of ES cells (38), was activated to a similar extent in both control and *EXT1*-deficient cells following treatment with LIF and FBS (Fig. 4, *A* and *B*). We observed comparable results in similar studies with E14TG2a cells (data not shown).

HS Chains Regulate Autocrine/Paracrine Wnt/β-Catenin Signaling in mES Cells—In the absence of feeder cells, we observed a significantly higher level of phosphorylation of β-catenin in *EXT1*-deficient cells than control cells (Fig. 5*A*). This suggests that there was a decrease in autocrine/paracrine Wnt/β-catenin signaling in *EXT1*-deficient cells. Next, we examined Wnt/β-catenin signaling using a luciferase reporter system. We found a significant decrease in luciferase activity in *EXT1*-deficient cells compared with control cells under feeder-free culture conditions (Fig. 5*B*). This is consistent with a reduction in autocrine/paracrine Wnt/β-catenin signaling in *EXT1*-deficient cells. We subsequently examined the nuclear localization of β-catenin, an indicator of activation of the canonical Wnt pathway. Accumulation of β-catenin was significantly decreased in the nuclei of *EXT1*-deficient cells compared with control cells (supplemental data 5). We carried out a Western blot analysis and confirmed that nuclear accumula-

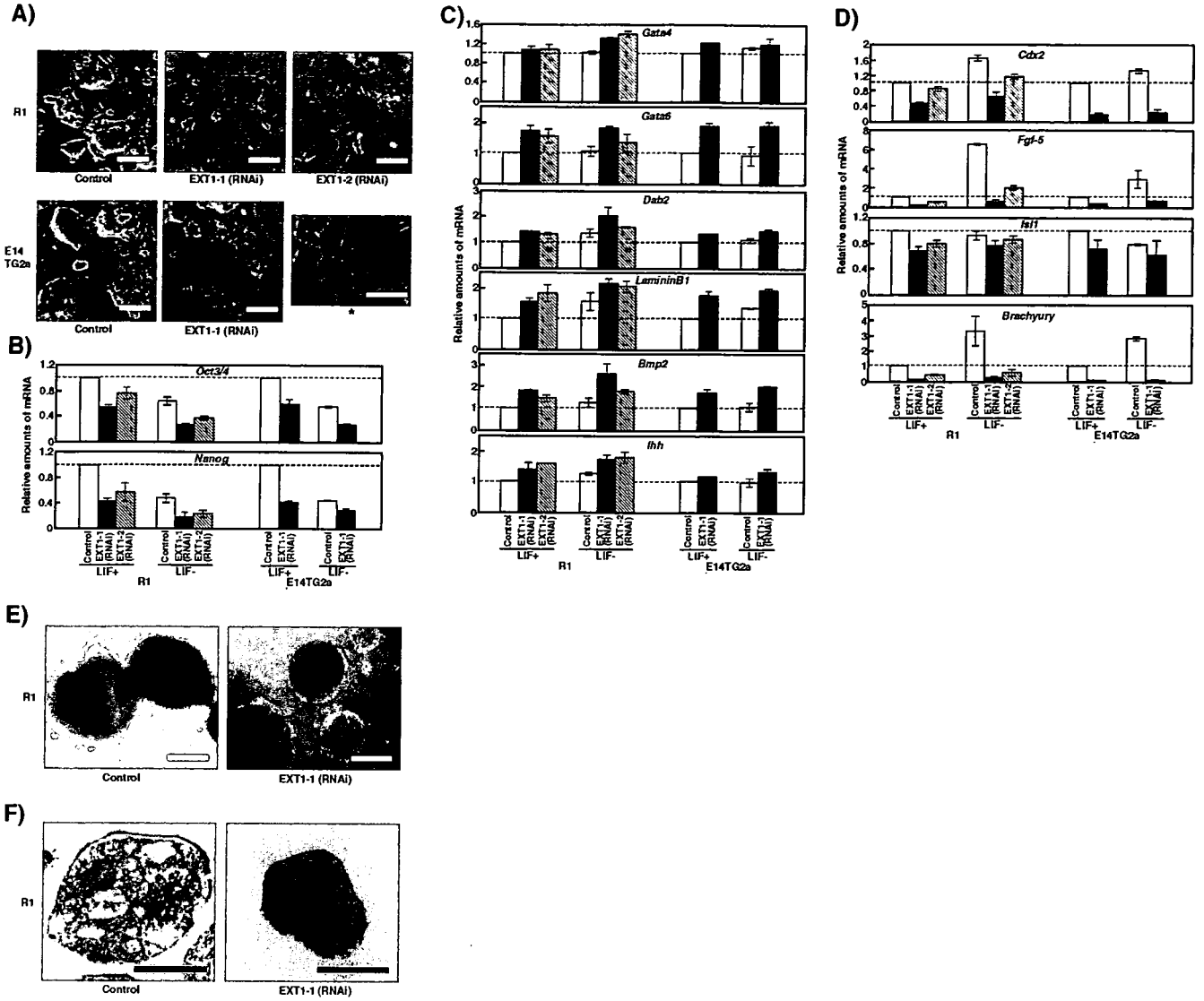

FIGURE 3. ***EXT1*-deficient cells differentiate spontaneously into the extraembryonic endoderm lineage.** *A*, photomicrographs of cells at 4 days after transfection in the presence of LIF. Representative photographs of control and *EXT1*-deficient cells from two independent experiments are shown. *Scale bars*, 100 μm. (*, high magnification image of the *boxed area* in *EXT1*-deficient R1 cells, stellate morphology of parietal endoderm. *Scale bars*, 50 μm). *B–D*, real time PCR analysis of cells 4 days after transfection in the presence or absence of LIF. The results are shown after normalization against control cells in the presence of LIF (value = 1). The values shown are the means ± S.D. from two independent experiments. *E*, representative photomicrographs at 6 days after EB formation. *Scale bars*, 200 μm. *F*, representative hematoxylin/eosin sections of EBs at 6 days after EB formation. *Scale bars*, 200 μm.

tion of β-catenin was reduced in *EXT1*-deficient cells compared with control cells (Fig. 5*C*). Thus, activation of Wnt/β-catenin signaling appeared to be reduced in *EXT1*-deficient cells. Similar results were observed in analogous studies using E14TG2a cells (data not shown).

RT-PCR analysis showed that both R1 and E14TG2a cell lines expressed several *Wnts*, as did MEFs. *Wnt2*, *Wnt4*, and *Wnt5a* were expressed in all cells, but *Wnt3a*, *Wnt7a*, and *Wnt10b* were expressed only in the mES cells (Fig. 5*D*). We examined the effect of reduction of HS chains on the ability of Wnt3a to bind to the mES cell surface. *EXT1*-deficient cells exhibited a significantly lower specific ^{125}I-Wnt3a binding than control cells (Fig. 5*E*), indicating that HS chains contribute to the binding of Wnt3a to the mES cell surface. Furthermore, SPR analysis (supplemental data 6) confirmed binding of Wnt3a to heparin, the structural analogue of HS chains, indicating that Wnt3a does indeed bind to HS chains on mES cells (apparent association and dissociation rate constants k_a (M^{-1} s^{-1}) and k_d (s^{-1}), 2.22×10^5, 5.77×10^{-3}, respectively, apparent equilibrium constant K_D (nM) for binding of Wnt3a to heparin, 26.0). These results demonstrate that HS chains regulate autocrine/paracrine Wnt/β-catenin signaling in mES cells.

HS Chain Regulation of Wnt/β-Catenin Signaling Contributes to Self-renewal of mES Cells—To determine whether the regulation of Wnt/β-catenin signaling by HS chains is necessary for the self-renewal and pluripotency of mES cells, we examined the effect of exogenous activation of Wnt/β-catenin signaling in *EXT1*-deficient cells using BIO, a specific pharmacological inhibitor of glycogen synthase kinase-3. The level of luciferase activity of Wnt/β-catenin signaling in BIO-treated

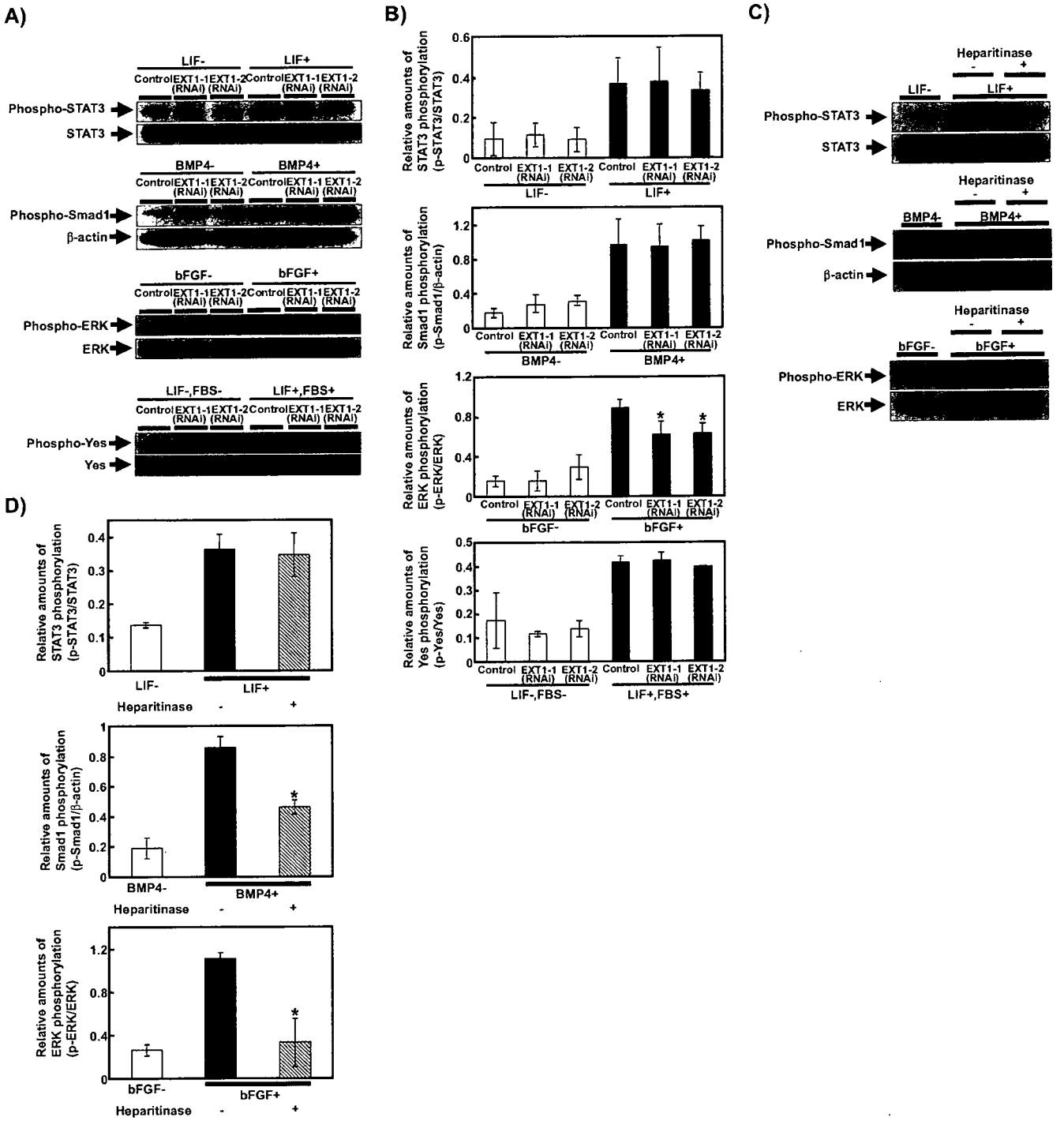

FIGURE 4. **Specific signaling is decreased in *EXT1*-deficient cells.** *A*, Western blot analysis of mES cells stimulated with each extrinsic factor. Two independent experiments were performed, and representative results are shown. *B*, quantification of Western blots shown in *A*. The *histograms* show mean densitometric readings ± S.D. of the phosphorylated protein/loading controls. Values were obtained from duplicate measurements of two independent experiments and significant values are indicated; *, $p < 0.01$, in comparison with stimulated control. *C*, Western blot analysis of mES cells stimulated with each extrinsic factor after treatment with or without heparitinase. Two independent experiments were performed, and representative results are shown. *D*, quantification of Western blots shown in *C*. The *histograms* show mean densitometric readings ± S.D. of the phosphoprotein/loading controls. Values were obtained from duplicate measurements of two independent experiments, and significant values are indicated; *, $p < 0.01$, in comparison with heparitinase untreated and extrinsically stimulated samples.

cells was 2–3-fold higher than in cells treated with MeBIO, an inactive analogue of BIO (data not shown). Two days after transfection, the level of *Nanog* mRNA was significantly up-regulated in BIO-treated cells (Fig. 6*A*), indicating that *Nanog* expression is regulated by Wnt/β-catenin signaling. The levels of *Nanog* and *Oct3/4* mRNAs in MeBIO-treated *EXT1*-deficient cells were 30–50% of those in MeBIO-treated control cells (Fig. 6*A*). Untreated cells showed similar results (data not

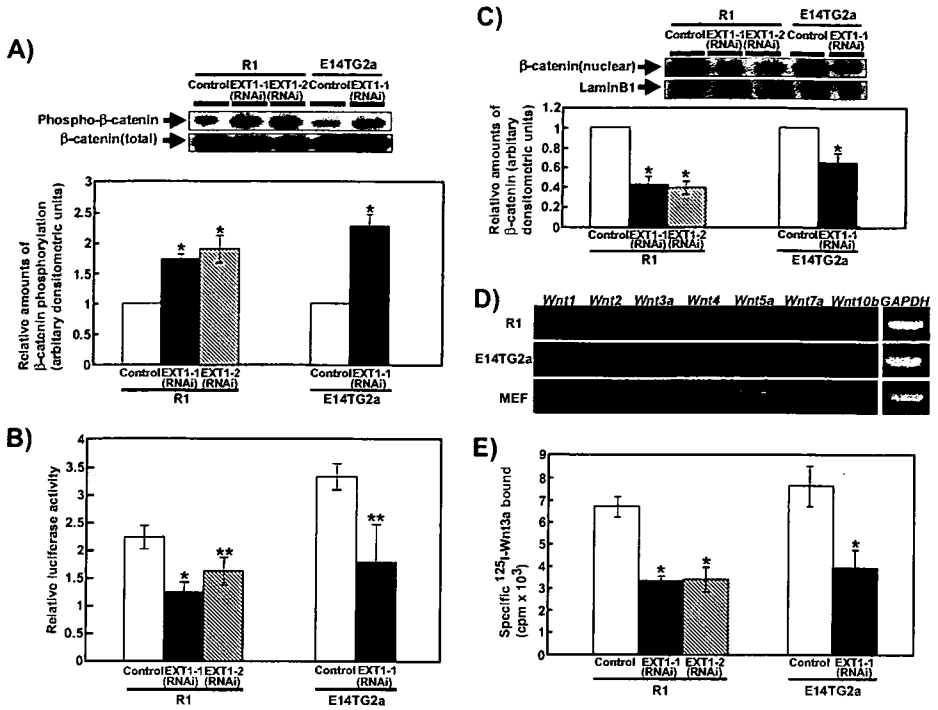

FIGURE 5. **Wnt/β-catenin signaling is decreased in *EXT1*-deficient cells.** *A*, Western blot analysis of mES cells after LIF and serum starvation for 4 h at 2 days after transfection. Representative immunoblots are shown. The *histograms* show mean densitometric readings ± S.D. of the phospho-β-catenin/total β-catenin after normalization against control cells (value = 1). Values were obtained from duplicate measurements of two independent experiments, and significant values are indicated; *, $p < 0.01$, in comparison with control. *B*, luciferase reporter assay. Relative luciferase activities (TOPFLASH/FOPFLASH) are shown as means ± S.D. from three independent experiments, and significant values are indicated; *, $p < 0.01$; **, $p < 0.05$, in comparison with control. *C*, Western blot analysis of mES cells at 3 days after transfection. Representative immunoblots are shown. The *histograms* show mean densitometric readings ± S.D. of the β-catenin/lamin B_1 after normalization against control cells (value = 1). Values were obtained from duplicate measurements of two independent experiments and significant values are indicated; *, $p < 0.01$, in comparison with control. *D*, RT-PCR analysis of the expression of several *Wnts* in mES cells and MEFs. *GAPDH*, glyceraldehyde-3-phosphate dehydrogenase. *E*, binding assay of ^{125}I-labeled Wnt3a. The value of specific ^{125}I-Wnt3a binding (total counts/min bound minus counts/min bound in the presence of 100 μg/ml free heparin) is the mean ± S.D. of three independent experiments, and significant values are indicated; *, $p < 0.01$, in comparison with control.

shown). This suggests that decreased signaling in *EXT1*-deficient cells affects the expression of *Nanog* and *Oct3/4*. BIO treatment rescued the level of *Nanog* mRNA in *EXT1*-deficient cells, but not of *Oct3/4* (Fig. 6*A*). The signaling pathways that regulate *Oct3/4* expression are therefore dependent upon HS chain expression but not upon Wnt. Furthermore, the expression patterns of Nanog and Oct3/4 proteins were correlated with mRNA levels (Fig. 6*B*). Recently, it has been demonstrated that the orphan nuclear receptor LRH-1 is required for maintenance of *Oct3/4* expression in mES cells (40). The level of *LRH-1* mRNA in *EXT1*-deficient cells treated with MeBIO was also reduced to 30–50% that in control cells (Fig. 6*A*), similarly to *Oct3/4* expression, but was unaffected by BIO treatment (Fig. 6*A*). This suggests that the reduction in *Oct3/4* expression in *EXT1*-deficient cells is mediated by LRH-1. Overall, our analyses demonstrate that Wnt/β-catenin signaling through HS chains regulates Nanog expression but not that of Oct3/4 in mES cells.

Next, we examined the ability of BIO to rescue self-renewal in *EXT1*-deficient cells. The number of AP-positive colonies derived from *EXT1*-deficient cells treated with MeBIO was significantly reduced compared with that of control cells (Fig. 6*C*). Nearly all of the colonies derived from culture of *EXT1*-deficient cells in the presence of BIO exhibited a tightly packed and AP-positive morphology reminiscent of undifferentiated ES cells cultured on a feeder layer. BIO treatment therefore rescued defective self-renewal in *EXT1*-deficient cells (Fig. 6*C*). This rescue effect demonstrates that HS chain-dependent signaling by Wnt/β-catenin contributes to self-renewal of mES cells. However, the total numbers of colonies scarcely differed between BIO-treated cells and MeBIO-treated cells (Fig. 6*C*), indicating that BIO treatment had no effect on cell proliferation. In a proliferation assay, we observed no effect of BIO on mES cell proliferation compared with untreated and MeBIO-treated cells (data not shown). These results demonstrate that HS chain-dependent signaling by autocrine/paracrine Wnt/β-catenin is required for the maintenance of self-renewal but not for the proliferation of mES cells.

Wnt/β-Catenin Signaling Regulated by HS Chains Is Important for Pluripotency of mES Cells—Our next step was to examine the effect of BIO on *EXT1*-deficient cell pluripotency in the absence of LIF, in which ES cells spontaneously differentiated into several lineages (Fig. 3, *B–D*). The expression of differentiation markers was analyzed 4 days after transfection using real time PCR analysis (Fig. 6, *D–F*). The expression of various differentiation markers was examined in *EXT1*-deficient cells treated with either BIO or MeBIO. BIO induced expression of the markers, including *Cdx2*, *Fgf-5*, and *Brachyury*; expression of the differentiation markers was at a low level in the MeBIO-treated cells. In the latter treatment group, only markers of the extraembryonic endoderm lineage (*Gata6*, *LamininB1*, and *BMP2*) were detected at appreciable levels (similar to those described in Fig. 3, *C* and *D*). Therefore, BIO rescued the defective pluripotency of *EXT1*-deficient cells.

Nanog-deficient mES cells spontaneously differentiate into the extraembryonic endoderm lineage, implicating Nanog in the control of mES cell pluripotency (14, 15). *Nanog* and *Oct3/4* expression was reduced in *EXT1*-deficient cells treated with MeBIO, whereas treatment with BIO rescued the level of *Nanog* expression although only to the same level as in MeBIO-treated control cells (Fig. 6*D*). Thus Wnt/β-catenin signaling sustains *Nanog* expression. In control cells, BIO treatment resulted in reduced expression of various differentiation markers associated with maintenance of *Nanog* and *Oct3/4* expression com-

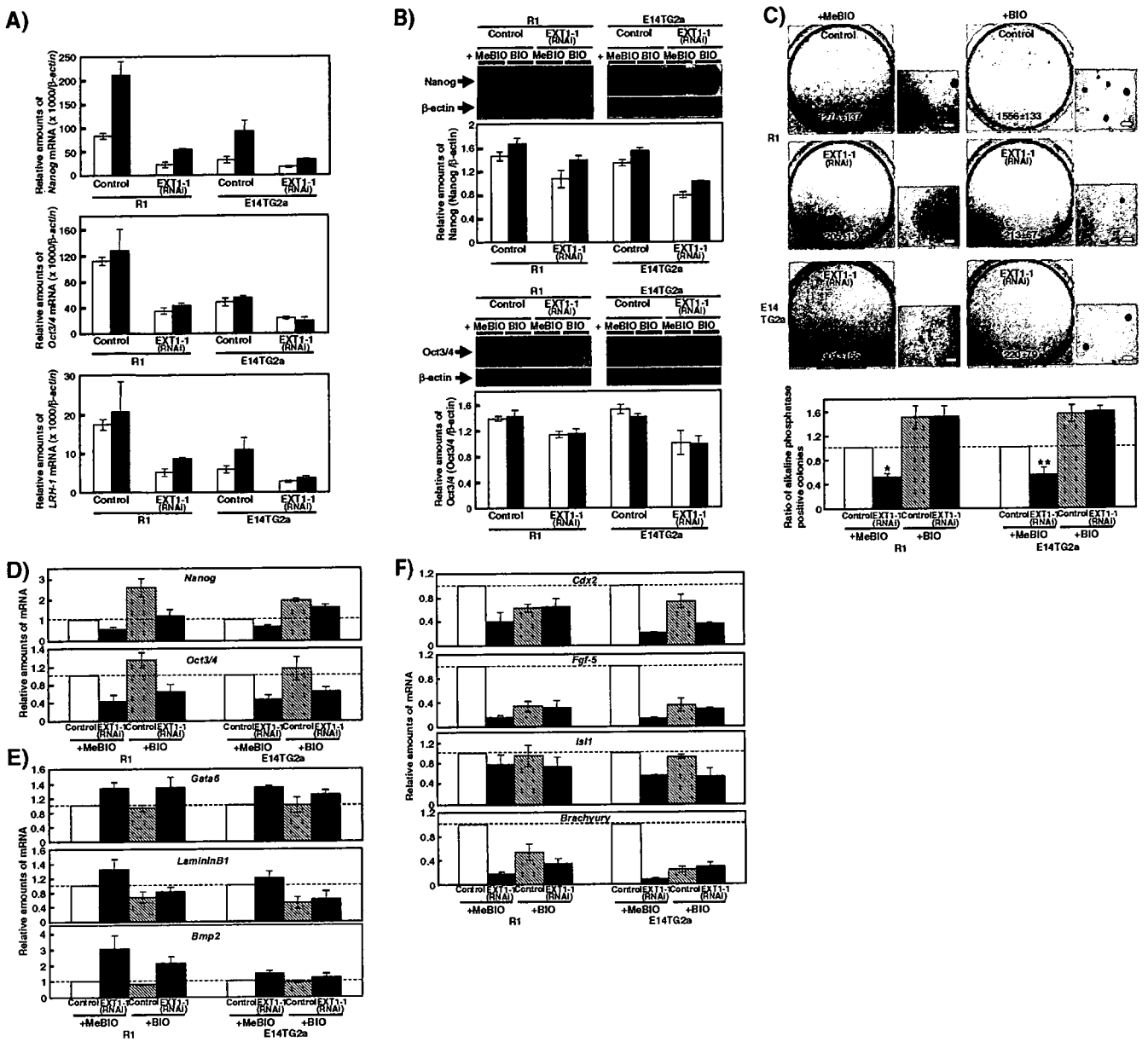

FIGURE 6. **Activation of Wnt/β-catenin signaling by treatment with BIO rescues self-renewal and pluripotency of *EXT1*-deficient cells.** *A*, real time PCR analysis of mES cells 2 days after transfection. The value shown is the mean ± S.D. of three independent experiments (*white bar*, MeBIO-treated; *black bar*, BIO-treated). *B*, Western blot analysis of mES cells at 2 days after transfection. Representative immunoblots are shown. The *histograms* show mean densitometric readings ± S.D. of the protein/β-actin. Values were obtained from duplicate measurements of two independent experiments (*white bar*, MeBIO-treated; *black bar*, BIO-treated). *C*, self-renewal assay. *Upper panels*, photographs of representative colonies. The total number of colonies is indicated at the *bottom* of each image. To the *right* of each photograph is a high magnification image. *Scale bars*, 200 μm. The ratio of AP-positive colonies is shown in *lower panels* after normalization against MeBIO-treated control cells (value = 1). The value shown is the mean ± S.D. of three independent experiments. Significant values are indicated; *, $p < 0.01$; **, $p < 0.03$, in comparison with control. *D–F*, real time PCR analysis of several germ layer markers at 4 days after transfection in the absence of LIF. The results are shown after normalization against MeBIO-treated control cells (value = 1). The values shown are the means ± S.D. of two independent experiments.

pared with MeBIO treatment. This indicates that BIO inhibited differentiation of control cells. In turn, maintenance of *Nanog* expression by autocrine/paracrine Wnt/β-catenin signaling through HS chains is important for the maintenance of pluripotency of mES cells.

DISCUSSION

In this study, we have demonstrated that *EXT1*-deficient mES cells, which express greatly reduced levels of HS chains, proliferate slowly and differentiate spontaneously into the extraembryonic endoderm lineage. Signaling by Wnt and FGF, but not BMP and LIF, was disrupted in *EXT1*-deficient cells. Furthermore, we demonstrated that autocrine/paracrine Wnt/β-catenin signaling through HS chains was necessary for maintenance of Nanog expression, self-renewal, and pluripotency in mES cells even in the presence of LIF/STAT3 and BMP/Smad signaling. Our results indicate that HS chains are important regulators of the extrinsic signaling

pathways contributing to self-renewal and pluripotency of mES cells.

We designed constructs expressing two different siRNAs targeting *EXT1*. Knockdown of *EXT1* in response to *EXT1-1* siRNA was maintained at ~20% of the level observed in control cells for at least 3 days following selection, even in the absence of puromycin. However, when *EXT1-2* siRNA was used, the level of *EXT1* mRNA recovered to 50–60% of that of control cells 3 days after selection (data not shown). As a result, the effects of *EXT1* knockdown were somewhat weaker in cells transfected with the *EXT1-2* plasmid (Figs. 2–5), reflecting a response that correlated with *EXT1* mRNA levels. These observations strongly support the conclusion that our results reflect the function of HS chains.

In this study, we used a transient knockdown system and found that the efficiency of knockdown decreased daily following the ending of selection. We therefore used puromycin to select for efficient knockdown in cells throughout the experiments described in Fig. 3 and Fig. 6, *D–F*. However, in the self-renewal and proliferation assays (Fig. 2 and Fig. 6*C*), the cells had to be replated at low densities, which rendered them susceptible to puromycin-induced cell death. Thus, puromycin could not be used after replating. These different conditions underlie the apparent experimental disparities such as that between Fig. 2*A*, in which undifferentiated colonies derived from *EXT1*-deficient cells were present at half of the level of control cells, and Fig. 3*A*, in which almost all *EXT1*-deficient cells differentiated.

Several signaling molecules, such as LIF/STAT3, BMP/Smad, Wnt/β-catenin, PI3K/Akt, and Src family members, are required for self-renewal of mES cells (7–12, 38, 39). Until now, it has been believed that extrinsic stimulation by both LIF and serum, including BMP, was sufficient to maintain mES cell self-renewal (4). However, in this study, we showed that self-renewal of mES cells was significantly decreased in response to the reduction in HS chain expression, even when LIF- and serum-mediated signaling were not reduced (Fig. 2 and Fig. 4). As shown in Fig. 5, several Wnts were expressed in mES cells, indicating that autocrine/paracrine Wnts function in mES cells. Indeed, autocrine/paracrine Wnt/β-catenin signaling was actually observed in cells cultured under feeder-free conditions. Furthermore, we showed that Wnt3a binds to the mES cell surface mediated by HS chains, and we demonstrated that autocrine/paracrine Wnt/β-catenin signaling through HS chains is important for maintenance of self-renewal of mES cells (Fig. 5 and Fig. 6). Thus, we propose that maintenance of mES cell self-renewal requires not only LIF plus serum factors but also autocrine/paracrine Wnts.

Reduction of HS chain expression also led to decreased signaling by FGF (Fig. 4). It has been demonstrated that HS chains regulate mouse fibroblast cell proliferation through FGF signaling (41). FGF has been also reported to maintain self-renewal of human ES cells (42), although this effect has yet to be observed in mES cells. We speculate that FGF signaling through HS chains may contribute to the maintenance of self-renewal and proliferation of mES cells, if FGF is present in serum or the conditioned medium. This idea is supported by the fact that HS chains have been shown to play crucial roles in FGF signaling during development (18).

We did not observe a reduction in BMP/Smad signaling in response to reduced short HS chains in mES cells (Fig. 4*B*), although previous reports have indicated that HS chains contribute to signaling by BMP in *Drosophila* and *Xenopus* (18, 43). The specific decrease in signaling by Wnt and FGF, but not by BMP, mediated by short HS chains in *EXT1*-deficient cells may be because of the effects of reduced HS chain length on the ability to accumulate sufficient ligands for their cognate receptors. This is supported by the result that HS chain depletion by heparitinase treatment led to not only further reduction in FGF signaling but also a reduction in BMP/Smad signaling (Fig. 4, *C* and *D*).

IL-6 is a heparin/HS-binding cytokine, and HS chains may regulate paracrine IL-6 signaling (44). Although LIF is an IL-6 family member and might also bind to HS chains, we demonstrated that HS chains are not required for LIF/STAT3 signaling. Neither reduction of HS chains (Fig. 4, *A* and *B*) nor HS chain depletion by heparitinase treatment (Fig. 4, *C* and *D*) had an effect on LIF/STAT3 signaling. Taken together, HS chains contribute to the regulation of several signaling pathways mediated by Wnt, BMP, and FGF but not LIF in mES cells (Fig. 7).

As shown in Fig. 6*C*, the total numbers of colonies scarcely differed between BIO-treated cells and MeBIO-treated cells, and we observed no effect of BIO on mES cell proliferation (data not shown), indicating that BIO treatment had no effect on cell proliferation. As shown in Fig. 2*B*, HS chains contribute to mES cell proliferation. Thus, we suggest that HS chain-mediated signaling pathways that are not influenced by Wnt/β-catenin control mES cell proliferation.

Nanog expression was increased in response to BIO treatment in both control and *EXT1*-deficient cells (Fig. 6*A*). However, the difference in the extent of increase in the expression of *Nanog* mRNA following BIO treatment of control and *EXT1*-deficient cells (Fig. 6*A*) indicates that other signaling pathways contribute to the control of its expression through HS chains. Recently, it has been demonstrated that *Nanog* transcription is regulated by an interaction between Oct3/4 and Sox2 or a novel pluripotential cell-specific Sox element-binding protein (45, 46). As such, the difference in the extent of the increase in the expression of *Nanog* mRNA following BIO treatment of control and *EXT1*-deficient cells may be due to a possible reduction in Oct3/4 and Sox2 or pluripotential cell-specific Sox element-binding protein mediated by unknown signaling through HS chains.

Expression of *Oct3/4* and *LRH-1* mRNA was decreased in *EXT1*-deficient cells treated with MeBIO (Fig. 6*A*), and their expression was not affected by BIO treatment in either control or *EXT1*-deficient cells (Fig. 6*A*). Thus regulation of *Oct3/4* and *LRH-1* expression does not require Wnt/β-catenin signaling through HS chains. LRH-1 has been shown to regulate the expression of *Oct3/4* by binding to its proximal enhancer and promoter (40). LRH-1 has also been shown to play an important role in the regulation of cell proliferation (47). The signaling pathways controlling the expression of LRH-1 remain to be determined. The decrease in *Oct3/4* expression observed in *EXT1*-deficient cells may be depend-

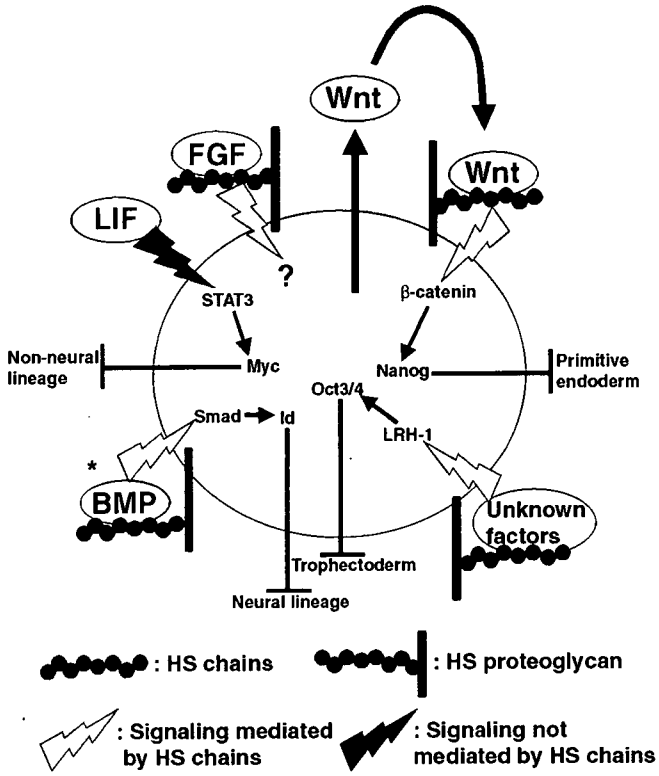

FIGURE 7. **HS chains regulate signaling by extrinsic factors required for the maintenance of self-renewal and pluripotency of mES cells.** HS chains contribute to the regulation of several signaling pathways mediated by extrinsic factors, such as BMP, Wnt, FGF, and unknown factors, but not to LIF and unknown serum factors in mES cells. We demonstrated that autocrine/paracrine Wnt/β-catenin signaling mediated by HS chains regulates Nanog expression and sustains self-renewal by suppression of primitive endodermal differentiation. BMP/Smad signaling is regulated by HS chains (Fig. 4, *C* and *D*) and blocks neural differentiation by induction of Id (11). FGF signaling is also regulated by HS chains (Fig. 4), but the signaling pathway required for maintenance of self-renewal is unknown in mES cells. From the observations made in this study, we suggest that HS chain-dependent signaling by unknown factors regulates mES cell proliferation and Oct3/4 expression. LIF/STAT3 signaling is not regulated by HS chains (Fig. 4) and blocks non-neuronal differentiation by induction of Myc (51). *, BMP/Smad signaling is not decreased by short HS chains (~35 kDa) but is decreased by depletion of HS chains.

ent upon the decrease in LRH-1 expression because of reduced signaling in these unidentified pathways in an HS chain-dependent manner. Although the signaling pathways activated downstream of HS chain expression remain to be determined, those required for LRH-1 expression might regulate the proliferation of mES cells.

In conclusion, we have demonstrated the importance of HS chains for the regulation of self-renewal and pluripotency of mES cells. These results suggest that it is possible to modify self-renewal and differentiation of ES cells by the use of RNAi targeted to genes encoding enzymes required for HS chain synthesis. Signaling by Wnt, FGF, and Notch have been shown to be involved in the regulation of self-renewal of hematopoietic and neural stem cells (48–50). However, the contribution of glycochains to such signaling in these cells has not yet been determined. Modulation of the glycosylation pathways in stem cells will provide the opportunity to engineer stem cells to follow specific differentiation programs that may be of use for the development of cell replacement therapies.

Acknowledgment—We thank Aya Juni for guiding ES cell culture.

REFERENCES

1. Evans, M. J., and Kaufman, M. H. (1981) *Nature* **292,** 154–156
2. Martin, G. R. (1981) *Proc. Natl. Acad. Sci. U. S. A.* **78,** 7634–7638
3. Thomson, J. A., Itskovitz-Eldor, J., Shapiro, S. S., Waknitz, M. A., Swiergiel, J. J., Marshall, V. S., and Jones, J. M. (1998) *Science* **282,** 1145–1147
4. Chambers, I., and Smith, A. (2004) *Oncogene* **23,** 7150–7160
5. Smith, A. G., Heath, J. K., Donaldson, D. D., Wong, G. G., Moreau, J., Stahl, M., and Rogers, D. (1988) *Nature* **336,** 688–690
6. Williams, R. L., Hilton, D. J., Pease, S., Willson, T. A., Stewart, C. L., Gearing, D. P., Wagner, E. F., Metcalf, D., Nicola, N. A., and Gough, N. M. (1988) *Nature* **336,** 684–687
7. Boeuf, H., Hauss, C., Graeve, F. D., Baran, N., and Kedinger, C. (1997) *J. Cell Biol.* **138,** 1207–1217
8. Matsuda, T., Nakamura, T., Nakao, K., Arai, T., Katsuki, M., Heike, T., and Yokota, T. (1999) *EMBO J.* **18,** 4261–4269
9. Niwa, H., Burdon, T., Chambers, I., and Smith, A. (1998) *Genes Dev.* **12,** 2048–2060
10. Raz, R., Lee, C. K., Cannizzaro, L. A., d'Eustachio, P., and Levy, D. E. (1999) *Proc. Natl. Acad. Sci. U. S. A.* **96,** 2846–2851
11. Ying, Q. L., Nichols, J., Chambers, I., and Smith, A. (2003) *Cell* **115,** 281–292
12. Sato, N., Meijer, L., Skaltsounis, L., Greengard, P., and Brivanlou, A. H. (2004) *Nat. Med.* **10,** 55–63
13. Wodarz, A., and Nusse, R. (1998) *Annu. Rev. Cell Dev. Biol.* **14,** 59–88
14. Chambers, I., Colby, D., Robertson, M., Nichols, J., Lee, S., Tweedie, S., and Smith, A. (2003) *Cell* **113,** 643–655
15. Mitsui, K., Tokuzawa, Y., Itoh, H., Segawa, K., Murakami, M., Takahashi, K., Maruyama, M., Maeda, M., and Yamanaka, S. (2003) *Cell* **113,** 631–642
16. Esko, J. D., and Selleck, S. B. (2002) *Annu. Rev. Biochem.* **71,** 435–471
17. Bernfield, M., Gotte, M., Park, P. W., Reizes, O., Fitzgerald, M. L., Lincecum, J., and Zako, M. (1999) *Annu. Rev. Biochem.* **68,** 729–777
18. Lin, X. (2004) *Development (Camb.)* **131,** 6009–6021
19. Bornemann, D. J., Duncan, J. E., Staatz, W., Selleck, S., and Warrior, R. (2004) *Development (Camb.)* **131,** 1927–1938
20. Han, C., Belenkaya, T. Y., Khodoun, M., Tauchi, M., and Lin, X. (2004) *Development (Camb.)* **131,** 1563–1575
21. Takei, Y., Ozawa, Y., Sato, M., Watanabe, A., and Tabata, T. (2004) *Development (Camb.)* **131,** 73–82
22. The, I., Bellaiche, Y., and Perrimon, N. (1999) *Mol. Cell* **4,** 633–639
23. Garcia-Garcia, M. J., and Anderson, K. V. (2003) *Cell* **114,** 727–737
24. Li, J. P., Gong, F., Hagner-McWhirter, A., Forsberg, E., Abrink, M., Kisilevsky, R., Zhang, X., and Lindahl, U. (2003) *J. Biol. Chem.* **278,** 28363–28366
25. Lin, X., Wei, G., Shi, Z., Dryer, L., Esko, J. D., Wells, D. E., and Matzuk, M. M. (2000) *Dev. Biol.* **224,** 299–311
26. Merry, C. L., Bullock, S. L., Swan, D. C., Backen, A. C., Lyon, M., Beddington, R. S., Wilson, V. A., and Gallagher, J. T. (2001) *J. Biol. Chem.* **276,** 35429–35434
27. Nagy, A., Rossant, J., Nagy, R., Abramow-Newerly, W., and Roder, J. C. (1993) *Proc. Natl. Acad. Sci. U. S. A.* **90,** 8424–8428
28. Smith, A. G., and Hooper, M. L. (1987) *Dev. Biol.* **121,** 1–9
29. Ui-Tei, K., Naito, Y., Takahashi, F., Haraguchi, T., Ohki-Hamazaki, H., Juni, A., Ueda, R., and Saigo, K. (2004) *Nucleic Acids Res.* **32,** 936–948
30. Toyoda, H., Kinoshita-Toyoda, A., and Selleck, S. B. (2000) *J. Biol. Chem.* **275,** 2269–2275
31. Suda, Y., Arano, A., Fukui, Y., Koshida, S., Wakao, M., Nishimura, T., Kusumoto, S., and Sobel, M. (2006) *Bioconjug. Chem.* **17,** 1125–1135
32. Wicklund, C. L., Pauli, R. M., Johnston, D., and Hecht, J. T. (1995) *Am. J. Med. Genet.* **55,** 43–46
33. Lind, T., Tufaro, F., McCormick, C., Lindahl, U., and Lidholt, K. (1998) *J. Biol. Chem.* **273,** 26265–26268
34. McCormick, C., Leduc, Y., Martindale, D., Mattison, K., Esford, L. E., Dyer, A. P., and Tufaro, F. (1998) *Nat. Genet.* **19,** 158–161
35. McCormick, C., Duncan, G., Goutsos, K. T., and Tufaro, F. (2000) *Proc. Natl. Acad. Sci. U. S. A.* **97,** 668–673

36. Senay, C., Lind, T., Muguruma, K., Tone, Y., Kitagawa, H., Sugahara, K., Lidholt, K., Lindahl, U., and Kusche-Gullberg, M. (2000) *EMBO Rep.* **1,** 282–286
37. Fujikura, J., Yamamoto, E., Yonemura, S., Hosoda, K., Masui, S., Nakao, K., Miyazaki Ji, J., and Niwa, H. (2002) *Genes Dev.* **16,** 784–789
38. Anneren, C., Cowan, C. A., and Melton, D. A. (2004) *J. Biol. Chem.* **279,** 31590–31598
39. Paling, N. R., Wheadon, H., Bone, H. K., and Welham, M. J. (2004) *J. Biol. Chem.* **279,** 48063–48070
40. Gu, P., Goodwin, B., Chung, A. C., Xu, X., Wheeler, D. A., Price, R. R., Galardi, C., Peng, L., Latour, A. M., Koller, B. H., Gossen, J., Kliewer, S. A., and Cooney, A. J. (2005) *Mol. Cell. Biol.* **25,** 3492–3505
41. Gallagher, J. T. (2001) *J. Clin. Investig.* **108,** 357–361
42. Xu, R. H., Peck, R. M., Li, D. S., Feng, X., Ludwig, T., and Thomson, J. A. (2005) *Nat. Methods* **2,** 185–190
43. Ohkawara, B., Iemura, S., ten Dijke, P., and Ueno, N. (2002) *Curr. Biol.* **12,** 205–209
44. Mummery, R. S., and Rider, C. C. (2000) *J. Immunol.* **165,** 5671–5679
45. Kuroda, T., Tada, M., Kubota, H., Kimura, H., Hatano, S. Y., Suemori, H., Nakatsuji, N., and Tada, T. (2005) *Mol. Cell. Biol.* **25,** 2475–2485
46. Rodda, D. J., Chew, J. L., Lim, L. H., Loh, Y. H., Wang, B., Ng, H. H., and Robson, P. (2005) *J. Biol. Chem.* **280,** 24731–24737
47. Botrugno, O. A., Fayard, E., Annicotte, J. S., Haby, C., Brennan, T., Wendling, O., Tanaka, T., Kodama, T., Thomas, W., Auwerx, J., and Schoonjans, K. (2004) *Mol. Cell* **15,** 499–509
48. Hitoshi, S., Alexson, T., Tropepe, V., Donoviel, D., Elia, A. J., Nye, J. S., Conlon, R. A., Mak, T. W., Bernstein, A., and van der Kooy, D. (2002) *Genes Dev.* **16,** 846–858
49. Panchision, D. M., and McKay, R. D. (2002) *Curr. Opin. Genet. Dev.* **12,** 478–487
50. Reya, T., and Clevers, H. (2005) *Nature* **434,** 843–850
51. Cartwright, P., McLean, C., Sheppard, A., Rivett, D., Jones, K., and Dalton, S. (2005) *Development (Camb.)* **132,** 885–896

BMCL 12488
21 January 2008 Disk used
ARTICLE IN PRESS
No. of Pages 6

Available online at www.sciencedirect.com
ScienceDirect
Bioorganic & Medicinal Chemistry Letters
ELSEVIER
Bioorganic & Medicinal Chemistry Letters xxx (2008) xxx–xxx

Sugar Chips immobilized with synthetic sulfated disaccharides of heparin/heparan sulfate partial structure☆

Masahiro Wakao,[a] Akihiro Saito,[a] Koh Ohishi,[a] Yuko Kishimoto,[b] Tomoaki Nishimura,[a,b] Michael Sobel[c] and Yasuo Suda[a,b,*]

[a]*Department of Nanostructure and Advanced Materials, Graduate School of Science and Engineering, Kagoshima University, 1-21-40 Korimoto, Kagoshima 890-0065, Japan*
[b]*SUDx-Biotec corporation, 5-5-2 Minatojima-cho, Kobe 650-0047, Japan*
[c]*Department of Surgery, University of Washington and VA Puget Sound Health Care System, Seattle, WA 98108, USA*

Received 21 August 2007; revised 24 December 2007; accepted 16 January 2008

Abstract—Carbohydrate chip technology has a great potential for the high-throughput evaluation of carbohydrate–protein interactions. Herein, we report syntheses of novel sulfated oligosaccharides possessing heparin and heparan sulfate partial disaccharide structures, their immobilization on gold-coated chips to prepare array-type Sugar Chips, and evaluation of binding potencies of proteins by surface plasmon resonance (SPR) imaging technology. Sulfated oligosaccharides were efficiently synthesized from glucosamine and uronic acid moieties. Synthesized sulfated oligosaccharides were then easily immobilized on gold-coated chips using previously reported methods. The effectiveness of this analytical method was confirmed in binding experiments between the chips and heparin binding proteins, fibronectin and recombinant human von Willebrand factor A1 domain (rh-vWf-A1), where specific partial structures of heparin or heparan sulfate responsible for binding were identified.

Carbohydrate chips and related array technologies[1–3] have attracted a great deal of attention as a powerful tool for glycomics. Like DNA[4] and protein chips,[5] they can rapidly and simply evaluate carbohydrate–protein interactions in parallel, with a minimum amount of sample. Our ongoing research involves this functional analysis of sulfated polysaccharides such as heparin (HP) and heparan sulfate (HS).[3a] HP and HS are highly sulfated polysaccharides and belong to the glycosaminoglycan (GAG) superfamily. They are among the most complex of carbohydrates, and play a significant role in biological processes through their binding interactions with numerous proteins,[6] such as growth factors, cytokines, viral proteins, and coagulation factors, among others. HP/HS have a basic structure composed of a repeating α or β(1,4)-linked disaccharide moiety which is derived from uronic acid (either glucuronic acid or iduronic acid) and *N*-acetyl-glucosamine residues. In general, HP/HS chains are very heterogeneous and contain innumerable substitution patterns due in part to some randomness in the multiple enzymatic modifications in their biosynthesis. This heterogeneity makes it difficult to elucidate the structure-function relationships of HP/HS at the molecular level. Therefore, structurally defined HP/HS sequences are necessary for the precise elucidation of the mode of HP/HS actions on their target molecules. So far, many synthetic efforts have been dedicated to the synthesis of HP/HS fragments.[3b–d,7,8]

Previously, we have reported that a specific disaccharide unit in HP, *O*-(2-deoxy-2-sulfamido-6-*O*-sulfo-α-D-glucopyranosyl)-(1-4)-2-*O*-sulfo-α-L-idopyranosyluronic acid (abbreviated as GlcNS6S-IdoA2S), is a key unit for binding to human platelets[9] and von Willebrand factor (vWf),[10] and that the clustering of these disaccharides significantly enhanced the interaction.[11,12] To systematically investigate heparin's binding properties, we have developed a method[3a] for the immobilization the sulfated oligosaccharide onto a gold-coated chip,

Keywords: Sugar; Carbohydrate; Chip; Heparin; Heparan sulfate; Carbohydrate–protein interaction; Surface plasmon resonance; SPR; SPR-imaging.
☆ Syntheses of sulfated oligosaccharide of heparin and heparan sulfate partial structures and their application to Sugar Chips are described.
* Corresponding author. Tel./fax: +81 99 285 8369; e-mail: ysuda@eng.kagoshima-u.ac.jp

0960-894X/$ - see front matter © 2008 Published by Elsevier Ltd.
doi:10.1016/j.bmcl.2008.01.069

and have devised an analytical system using surface plasmon resonance (SPR) technology, which permits their real-time study without further labeling. These systems can be applied to the investigation of the binding interactions of a variety of structurally defined oligosaccharides.

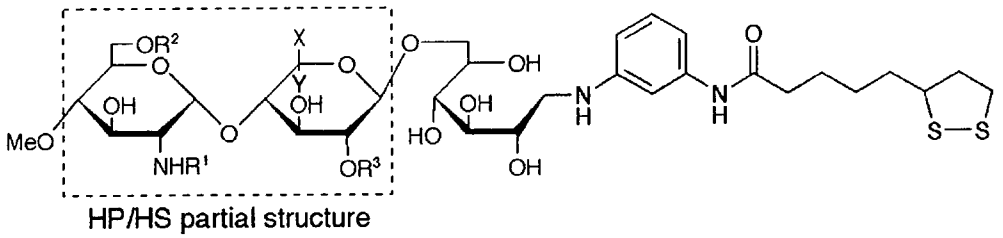

1, GlcNS6S-IdoA2S: $R^1=SO_3^-$, $R^2=SO_3^-$, $R^3=SO_3^-$, X=H, $Y=CO_2^-$
2, GlcNS-IdoA2S: $R^1=SO_3^-$, R^2=H, $R^3=SO_3^-$, X=H, $Y=CO_2^-$
3, GlcNS6S-GlcA: $R^1=SO_3^-$, $R^2=SO_3^-$, R^3=H, $X=CO_2^-$, Y=H
4, GlcNS-GlcA: $R^1=SO_3^-$, R^2=H, R^3=H, $X=CO_2^-$, Y=H

Figure 1. Sulfated disaccharide partial structures of heparin/heparan sulfate.

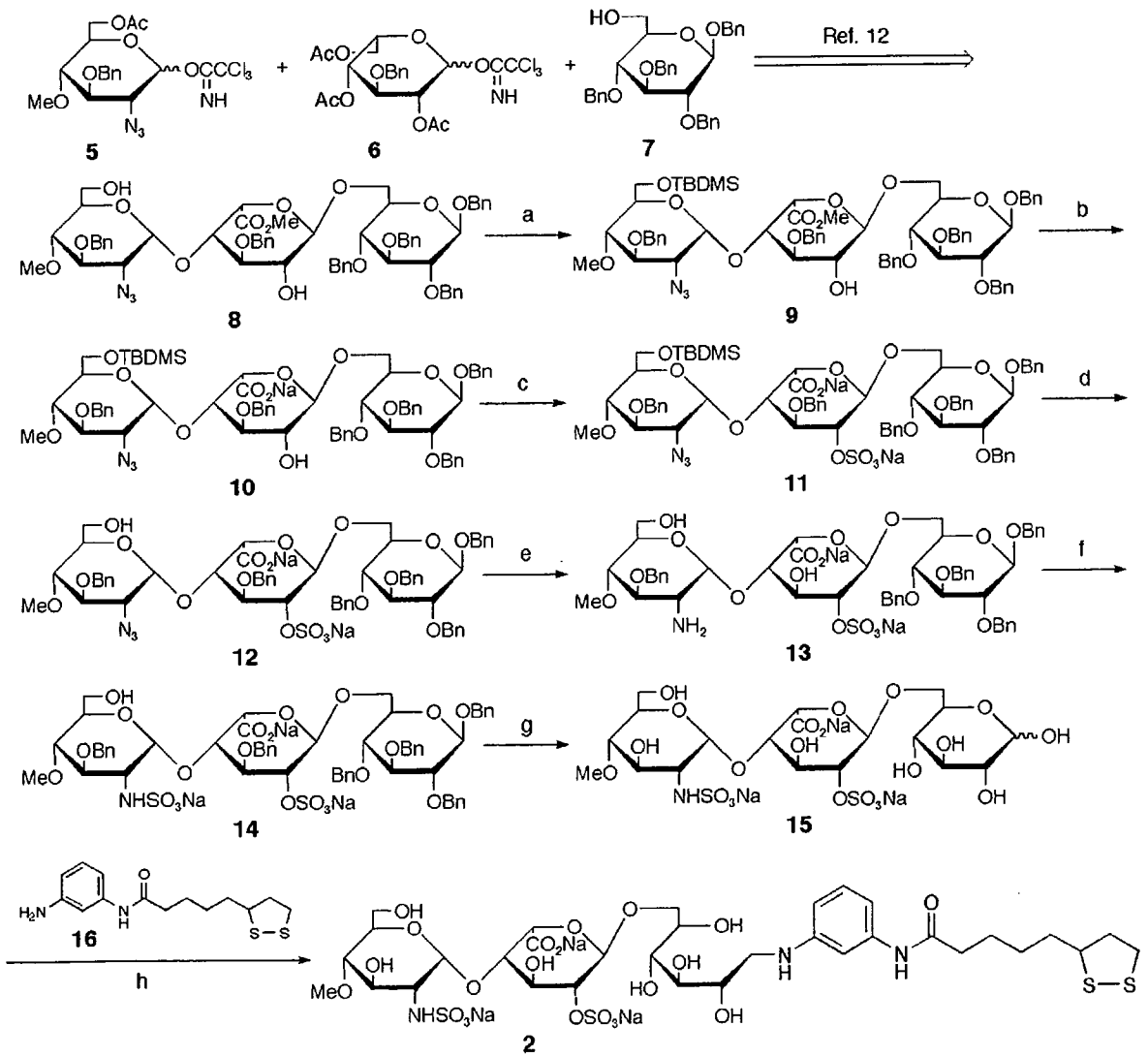

Scheme 1. Synthesis of ligand conjugate **2** containing GlcNS-IdoA2S. Reagents: (a) TBDMSCl, imidazole, MS4AP in CH_2Cl_2, 45%; (b) 1 M NaOH, MeOH/THF (1:1), 70%; (c) SO_3Pyr in Pyr; (d) HFPyr in Pyr; (e) 10% Pd–C, H_2 (1 kg/cm^2) in THF/MeOH (2:1); (f) SO_3Pyr in H_2O; (g) 10% Pd–C, H_2 (7 kg/cm^2) in H_2O/AcOH (5:1), 29% (5 steps); (h) $NaBH_3CN$ in DMAc/H_2O/AcOH (1:1:0.1), 82%.

Please cite this article in press as: Wakao, M. et al., *Bioorg. Med. Chem. Lett.* (2008), doi:10.1016/j.bmcl.2008.01.069

To better understand the HP/HS disaccharide structures involved in specific protein interactions, we designed three kinds of sulfated trisaccharide ligand conjugates **2–4** containing the disaccharide units as shown in Figure 1; GlcNS-IdoA2S (**2**): *O*-(2-deoxy-2-sulfamido-α-D-glucopyranosyl)-(1-4)-2-*O*-sulfo-α-L-idopyranosyluronic acid, GlcNS6S-GlcA (**3**): *O*-(2-deoxy-2-sulfamido-6-*O*-sulfo-α-D-glucopyranosyl)-(1-4)-α-D-glucopyranosyluronic acid, GlcNS-GlcA (**4**): *O*-(2-deoxy-2-sulfamido-α-D-glucopyranosyl)-(1-4)-α-D-glucopranosyluronic acid. The disaccharide units contained in ligand conjugates **1–4** of Figure 1 are frequently found in HP/HS disaccharide unit.

For efficient synthesis, four monomeric building blocks were prepared. 2-Azido glucose derivative **5**, idose derivative **6**, and 4,6-benzylidene glucose derivative **17** were used for glucosamine, iduronic acid, and glucuronic acid moieties, respectively. Selective sulfation onto glucosamine and iduronic acid or glucuronic acid moieties can be carried out by an appropriate functionalization. The 6-OH glucose derivative **7** was used as the reducing end for the conjugation to linker molecule **16** after deprotection on the glucose, which works not only as a reducing end donor for reductive amination but also as the hydrophilic moiety in the molecule to minimize any non-specific hydrophobic interactions between the linker and target proteins or cells.

The synthesis of ligand conjugate **2** containing GlcNS-IdoA2S unit was carried out as shown in Scheme 1. Trisaccharide **8**, which was prepared according to the method reported previously,[12] was selectively protected by *t*-butyldimethylsilyl (TBDMS) group. The methyl ester of trisaccharide **9** was hydrolyzed and the remaining 2′-hy-

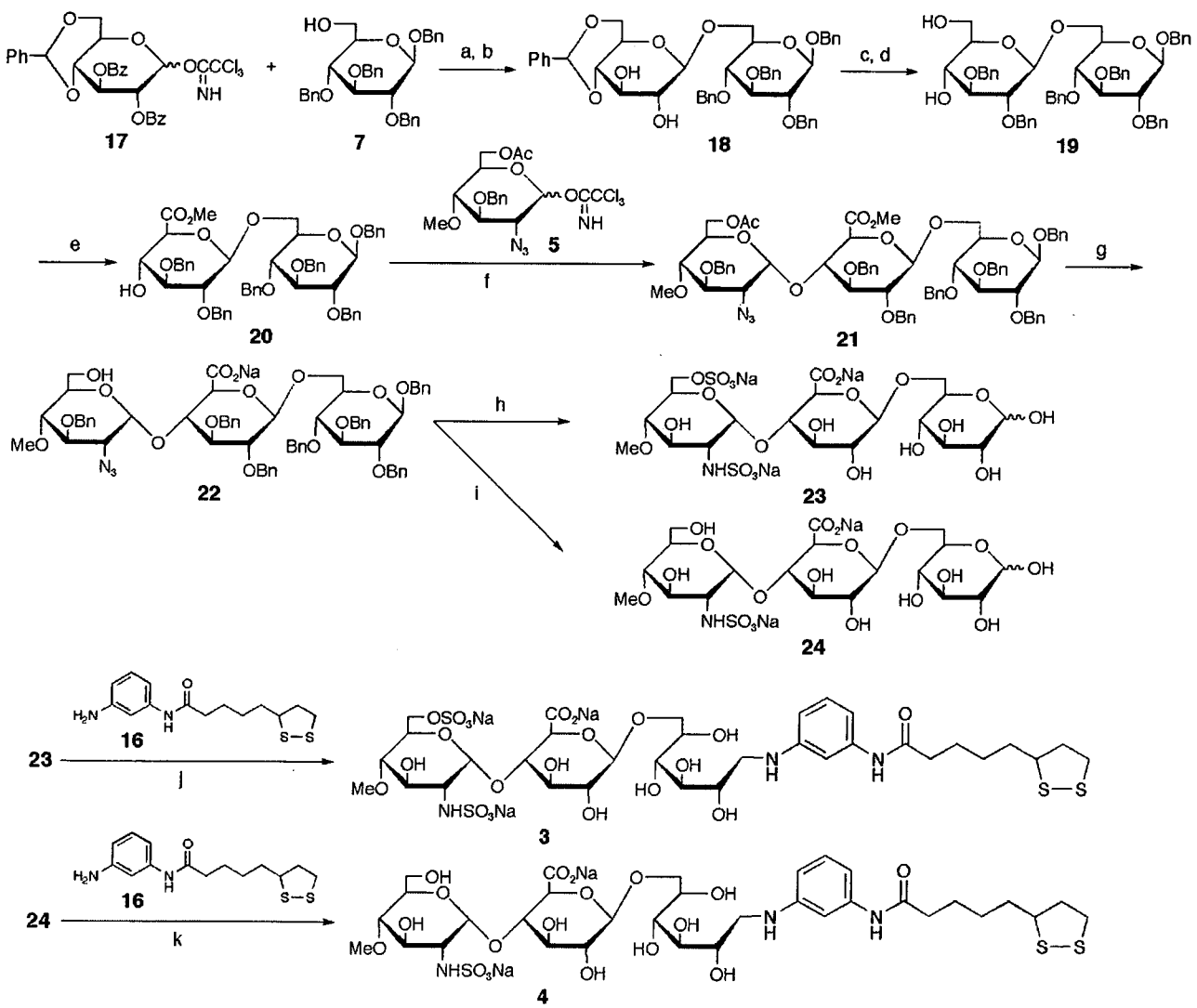

Scheme 2. Synthesis of ligand conjugates **3** and **4** containing GlcNS6S-GlcA and GlcNS-GlcA, respectively. Reagents and conditions: (a) BF_3OEt_2, MS4AP in CH_2Cl_2, −20 °C; (b) 0.1 M NaOMe, 90% (2 steps); (c) NaH, BnBr in DMF, 0 °C → rt, 88%; (d)16% TFA, 8% MeOH in CH_2Cl_2, 0 °C → rt, 93%; (e) TEMPO, KBr, NaClO in CH_2Cl_2; $TMSCHN_2$, 83% (2 steps); (f) TBDMSOTf, MS4AP in toluene, −20 °C, 84%; (g) 5 M NaOH in MeOH/THF (1:1), 89%; (h) SO_3Pyr in Pyr; 10% Pd–C, H_2 (1 kg/cm^2) in THF/H_2O (2:1); SO_3Pyr in H_2O (pH ≈ 9.5); 10% Pd–C, H_2 (7 kg/cm^2) in H_2O/AcOH (5:1), 28% (4 steps); (i) 10% Pd–C, H_2 (1 kg/cm^2) in THF/H_2O (2:1); SO_3Pyr in MeOH/H_2O (3:2); 10% Pd–C, H_2 (7 kg/cm^2) in H_2O/MeOH/AcOH (5:5:2), 39% (3 steps); (j) $NaBH_3CN$ in DMAc/H_2O/AcOH (1:1:0.1), 62%; (k) $NaBH_3CN$ in DMAc/H_2O/AcOH (1:1:0.1), 50%.

Please cite this article in press as: Wakao, M. et al., *Bioorg. Med. Chem. Lett.* (2008), doi:10.1016/j.bmcl.2008.01.069

droxy group was sulfated using sulfur trioxide-pyridine complex at room temperature. After removing the TBDMS group with HFpyridine complex, the azido group was reduced using a catalytic amount of Pd-C under hydrogen atmosphere and the resulting amino group was *N*-sulfated. All benzyl protecting groups were removed by hydrogenolysis using catalytic Pd-C to give the desired trisaccharide **15**. Finally, the reductive amination of trisaccharide **15** with linker compound **16** was performed using $NaBH_3CN$ to afford the desired ligand conjugate **2** in good yield. Compound **2** was purified by gel-filtration chromatography with Sephadex G-25 fine and confirmed by ^1H NMR and ESI-TOF/MS analyses.[13]

The syntheses of ligand conjugates **3** and **4** were carried out in the same fashion as the syntheses of **1** and **2** (Scheme 2). Glycosylation of 6-OH glucose **7** and imidate **17** with trimethylsilyl trifluoromethanesulfonate (TMSOTf) as a promoter and treatment of the resultant with NaOMe gave disaccharide **18** in a good yield. The resulting hydroxy groups of **18** were then protected with a benzyl group. After removal of the benzylidene group, the primary 6′-OH group was selectively oxidized to carboxylic acid using 2,2,6,6-tetramethyl-1-piperidinyloxy (TEMPO).[14] The resulting carboxyl group was esterified with (trimethylsilyl)diazomethane to afford the disaccharide **20**. The 2-azido imidate **5** was condensed with disaccharide **20** using TBDMSOTf at −20 °C to give selectively an α-linked trisaccharide **21**.[11,15] Hydrolysis of the acetyl group and methyl ester was then carried out using aqueous NaOH to give the common intermediate **22** for trisaccharides **23** and **24**. The sulfated trisaccharide **23** was obtained by *O*-sulfation of the 6″-hydoxyl group and reduction and *N*-sulfation of 2′-azido group was followed by hydrogenolysis. Conversely, the sulfated trisaccharide **24** was prepared by the same method as the synthesis of trisaccharide **23**, omitting the *O*-sulfation. The ligand-conjugates **3**[16] and **4**[17] were synthesized in satisfactory yields as similar to the described procedure for compound **2**.

Binding interactions were investigated by use of the SPR imaging sensor.[18] When fibronectin was tested (Fig. 2), specific binding interactions were clearly observed with compounds **1** (GlcNS6S-IdoA2S, K_D = 5.5 nM) and **3** (GlcNS6S-GlcA, K_D = 6.5 nM), but not with compounds **2** (GlcNS-IdoA2S, K_D = 30 nM) and **4** (GlcNS-GlcA, K_D = 33 nM). These results indicate that the *N*-sulfation and 6-*O*-sulfation of glucosamine in HP/HS are important for fibronectin binding, while 2-*O*-sulfation of iduronic acid is less important. Recently,

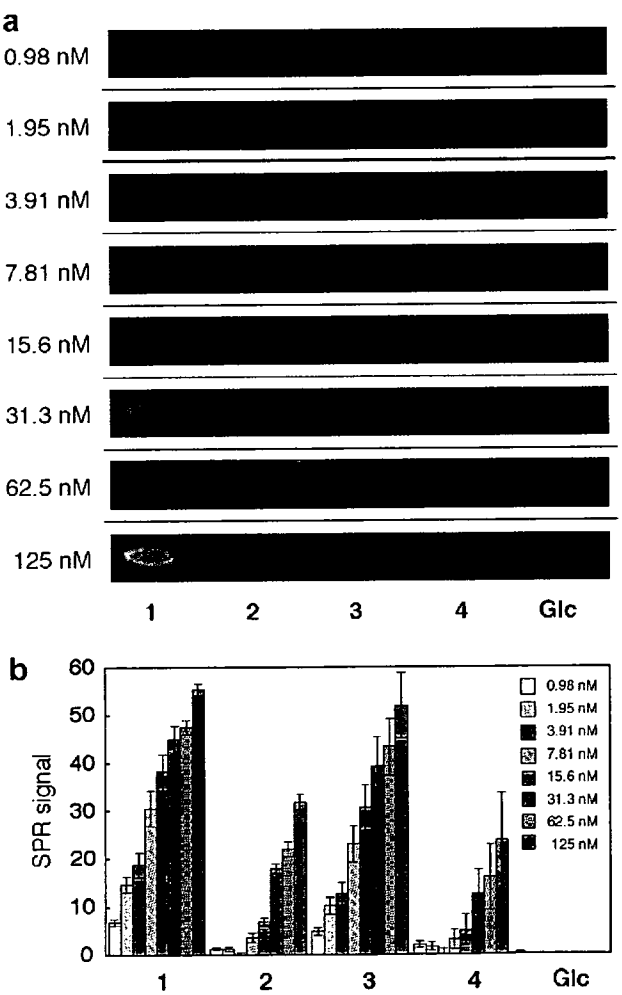

Figure 2. Binding study with fibronectin. (a) SPR difference imaging on the chip immobilized with compounds **1**, **2**, **3**, **4**, and Glcα(1-6)Glc-mono (Glc). Measurements were carried out with analyte in the range between 0.98 and 125 nM. (b) Bar graph profiles of different concentrations of protein. The error bars represent +/− SEM.

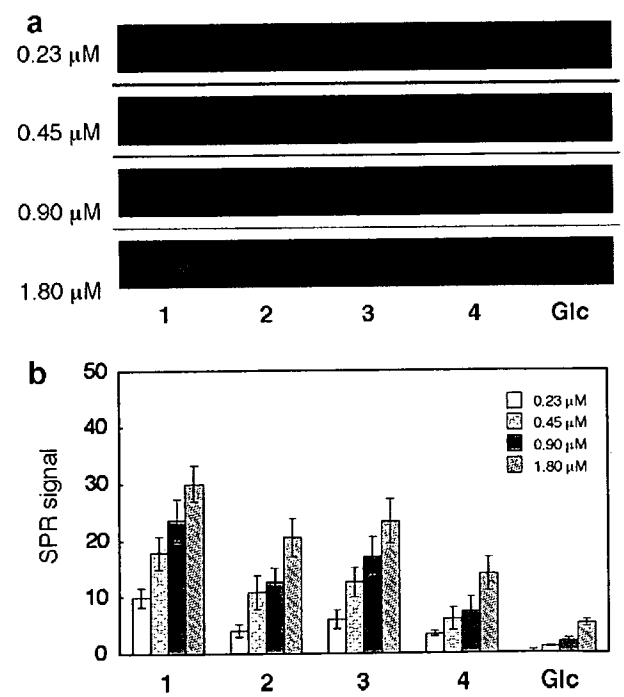

Figure 3. Binding study with rh-vWf-A1. (a) SPR difference imaging on the chip immobilized with compounds **1**, **2**, **3**, **4**, and Glcα(1-6)Glc-mono (Glc). Measurements were carried out with analyte in the range between 0.23 and 1.80 μM. (b) Bar graph profiles of different concentrations. The error bars represent +/− SEM.

Couchman and coworkers showed that *N* -sulfation of glucosamine was essential for fibronectin binding and 2-*O*-sulfation of iduonic acid or 6-*O*-sulfation of glucosamine has marginal effects.[19] Additionally, *N*-sulfation and 6-*O*-sulfation of glucosamine were important for focal adhesion formation through syndecan-4, heparan sulfate proteoglycan. Our results are in agreement with those data.

In contrast, when recombinant human vWf A1 domain (rh-vWf-A1)[20] was injected over the chips, a different pattern of oligosaccharide binding preference was noted (Fig. 3). A strong interaction was observed with compounds **1** (GlcNS6S-IdoA2S, K_D = 1.0 μM) and **2** (GlcNS-IdoA2S, K_D = 0.9 μM). Weaker interaction was seen with compound **3** (GlcNS6S-GlcA, K_D = 1.4 μM), while distinctly low binding was observed with compound **4** (GlcNS-GlcA, K_D = 4.3 μM). Although the GlcNS6S-IdoA2S (**1**) disaccharide structure was considered a key binding domain of vWf,[10] the exact disaccharide structure responsible for vWf binding is still unclear. We found previously that clustered compounds containing three units of GlcNS6S-IdoA2S[12] possessed higher competitive binding activity compared to compounds containing less than two units of GlcNS6S-IdoA2S (unpublished data). Together with those data, the current results indicate that the tri-sulfated disaccharide binds vWf best, that loss of either the 6-sulfate of GlcN or the 2-sulfate of Ido reduces vWf binding significantly, and that the *N*-sulfate of GlcN alone is not sufficient for binding vWf.

In conclusion, we have designed new, precisely sulfated oligosaccharides of HP/HS partial structures. These oligosaccharides were efficiently synthesized using appropriate monosaccharide intermediates. Their application in an array type Sugar Chip, using SPR imaging analysis has been shown to be an efficient and specific technology to elucidate the interactions between a protein and multiple sulfated disaccharides, on a real time scale. These techniques can be used for high-throughput screening of protein samples, as well as for solving the structure–function relations of an individual protein–glycosaminoglycan interaction at the molecular and nanoscale.

Acknowledgments

The present work was financially supported in parts by grants from Japan Science and Technology Agency (Pre-venture program to Y.S., CREST to Y.S.), the National Institutes of Health (Grant HL079182 to M.S. and the Department of Veterans Affairs Research Service (to M.S.).

Supplementary data

Supplementary data associated with this article can be found, in the online version, at doi:10.1016/j.bmcl.2008.01.069.

References and notes

1. For reviews, see: (a) Love, K. R.; Seeberger, P. H. *Angew. Chem. Int. Ed.* **2002**, *41*, 3583; (b) Feizi, T.; Fazio, F.; Chai, W.; Wong, C. H. *Curr. Opin. Struct. Biol.* **2003**, *13*, 637; (c) Wang, D. *Proteomics* **2003**, *3*, 2167; (d) Shin, I.; Park, S.; Lee, M. *Chem. Eur. J.* **2005**, *11*, 2894; (e) Ortiz Mellet, C.; Garcia Fernandez, J. M. *ChemBioChem* **2002**, *3*, 819.
2. For articles, see: (a) Blixt, O.; Head, S.; Mandala, T.; Scanlan, C.; Hufflejt, M. E.; Alvarez, R.; Bryan, M. C.; Fazio, F.; Calarese, D.; Stevens, J.; Razi, N.; Stevens, D. J.; Skehel, J. J.; van Die, I.; Burton, D. R.; Wilson, I. A.; Cummings, R.; Bovin, N.; Wong, C. H. *Proc. Natl. Acad. Sci. U.S.A.* **2004**, *101*, 17033; (b) Chevolet, Y.; Martins, J.; Milosevic, N.; Léonard, D.; Zeng, S.; Malissard, M.; Berger, E. G.; Maier, P.; Mathieu, H. J.; Crout, D. H. G.; Sigrist, H. *Bioorg. Med. Chem.* **2001**, *9*, 2943; (c) Park, S.; Lee, M. R.; Pyo, S. J.; Shin, I. *J. Am. Chem. Soc.* **2004**, *126*, 4812; (d) Burn, M. A.; Disney, M. D.; Seeberger, H. P. *ChemBioChem* **2006**, *7*, 421; (e) Houseman, B. T.; Mrksich, M. *Chem. Biol.* **2002**, *9*, 443; (f) Fazio, F.; Bryan, M. C.; Blixt, O.; Paulson, J. C.; Wong, C. H. *J. Am. Chem. Soc.* **2002**, *124*, 14397; (g) Lee, M.; Shin, I. *Angew. Chem. Int. Ed.* **2005**, *44*, 2881; (h) Schwarz, M.; Spector, L.; Gargir, A.; Shtevi, A.; Gortler, M.; Altstock, R. T.; Dukler, A. A.; Dotan, N. *Glycobiology* **2003**, *13*, 749; (i) Zhou, X. C.; Zhou, J. H. *Biosens. Bioelectron.* **2006**, *21*, 1451; (j) Manimala, J. C.; Roach, T. A.; Li, Z. T.; Gildersleeve, J. C. *Angew. Chem. Int. Ed.* **2006**, *45*, 3607; (k) Wang, D.; Liu, S.; Trummer, B. J.; Deng, C. *Nat. Biotechnol.* **2002**, *20*, 275; (l) Chevolet, Y.; Bouillon, C.; Vidal, S.; Morvan, F.; Meyer, A.; Cloarec, J. J.; Jochum, A.; Parly, J. P.; Vasseur, J. J.; Souteyrand, E. *Angew. Chem. Int. Ed.* **2007**, *46*, 2398.
3. Recent carbohydrate chips immobilized sulfated oligosaccharide, see: (a) Suda, Y.; Arano, A.; Fukui, Y.; Koshida, S.; Wakao, M.; Nishimura, T.; Kusumoto, S.; Sobel, M. *Bioconjugate Chem.* **2006**, *17*, 1125; (b) de Paz, J. L.; Noti, C.; Seeberger, P. H. *J. Am. Chem. Soc.* **2006**, *128*, 2766; (c) de Paz, J. L.; Spillmann, D.; Seeberger, P. H. *Chem. Commun.* **2006**, 3116; (d) Noti, C.; de Paz, J. L.; Polito, L.; Seeberger, P. H. *Chem. Eur. J.* **2006**, *12*, 8664; (e) Tully, S. E.; Rawat, M.; Hsieh-Wilson, L. C. *J. Am. Chem. Soc.* **2006**, *128*, 7740.
4. (a) Perou, C. M. *Nature* **2000**, *406*, 747; (b) Ramsey, G. *Nat. Biotechnol.* **1998**, *16*, 40; (c) Marshall, A.; Hodgson, J. *Nat. Biotechnol.* **1998**, *16*, 27; (d) DeRisi, J. L.; Lyer, V. R.; Brown, P. O. *Science* **1997**, *278*, 680.
5. (a) Templin, M. F.; Stoll, D.; Schrenk, M.; Traub, P. C.; Vchringer, C. F.; Joos, T. O. *Trends Biotechnol.* **2002**, *20*, 160; (b) Weinberger, S. R.; Dalmasso, E. A.; Fung, E. T. *Curr. Opin. Chem. Biol.* **2002**, *6*, 86; (c) Fung, E. T.; Thulasiraman, V.; Weinberger, S. R.; Dalmasso, E. A. *Curr. Opin. Biotechnol.* **2001**, *12*, 65; (d) Zhu, H. *Science* **2001**, *293*, 2101; (e) MacBeath, G.; Schreiber, S. L. *Science* **2000**, *289*, 1760.
6. (a) Conrad, H. E. *Heparin-Binding Proteins*; Academic Press: San Diego, 1998; (b) Capila, I.; Lindhardt, R. J. *Angew. Chem. Int. Ed.* **2002**, *41*, 390; (c) Turnbull, J.; Powell, A.; Guimond, S. *Trends Cell Biol.* **2001**, *11*, 75; (d) Bernfield, M.; Götte, M.; Park, P. W.; Reizes, O.; Fitzgerald, M. L.; Lincecum, J.; Zako, M. *Annu. Rev. Biochem.* **1999**, *68*, 729; (e) Rabenstein, D. A. *Nat. Prod. Rep.* **2002**, *19*, 312; (f) Casu, B.; Lindahl, U. *Adv. Carbohydr. Chem. Biochem.* **2001**, *57*, 159.
7. For comprehensive review on the synthesis on GAGs, see: Yeung, B. K. S.; Chong, P. Y. C.; Petillo, P. A. *J. Carbohydr. Chem.* **2002**, *21*, 799.

8. Recent articles, see: (a) Lu, L.-D.; Shie, C.-R.; Kulkarni, S. S.; Pan, G.-R.; Lu, X.-A.; Hung, S.-C. *Org. Lett.* **2006**, *8*, 5995; (b) Zhou, Y.; Lin, F.; Chen, J.; Yu, B. *Carbohydr. Res.* **2006**, *341*, 1619; (c) Codée, J. D. C.; Stubba, B.; Schiattarella, M.; Overkleeft, H. S.; van Boeckel, C. A. A.; van Boom, J. H.; van der Marel, G. A. *J. Am. Chem. Soc.* **2005**, *127*, 3767, And references are therein.
9. (a) Suda, Y.; Marques, D.; Kermode, J. C.; Kusumoto, S.; Sobel, M. *Thromb. Res.* **1993**, *69*, 501; (b) Suda, Y.; Bird, K.; Shiyama, T.; Koshida, S.; Marques, D.; Fukase, K.; Sobel, M.; Kusumoto, S. *Tetrahedron Lett.* **1996**, *37*, 1053.
10. Poletti, L. F.; Bird, K. E.; Marques, D.; Harris, R. B.; Suda, Y.; Sobel, M. *Arterioscler. Thromb. Vasc. Biol.* **1997**, *17*, 925.
11. Koshida, S.; Suda, Y.; Fukui, Y.; Ormsby, J.; Sobel, M.; Kusumoto, S. *Tetrahedron Lett.* **1999**, *40*, 5725.
12. Koshida, S.; Suda, Y.; Sobel, M.; Kusumoto, S. *Tetrahedron Lett.* **2001**, *42*, 1289.
13. Spectral data for compound **2**: ^{1}H NMR (600 MHz, D_2O), δ 7.11 (1 H, t, J = 7.9 Hz), 6.77–6.75 (2 H, m), 6.58 (1H, d, J = 7.9 Hz), 5.22 (1H, d, J = 3.4 Hz), 4.97 (1H, brs), 4.14 (1H, brs), 4.05 (1H, brs), 3.92 (1H, brs), 3.82–3.71 (2H, m), 3.70–3.61 (5H, m), 3.59–3.55 (5H, m), 3.38 (3H, s), 3.28 (1H, dd, J = 9.6 and 3.4 Hz), 3.16 (1H, dd, J = 9.6 and 10.3 Hz), 3.09–3.00 (4H, m), 2.34–2.31 (1H, m), 2.27 (2H, t, J = 6.9), 1.87-1.83 (1H, m), 1.63–1.50 (4H, m), 1.37–1.33 (2H, m), ESI-MS (negative mode); Found: *m/z* 484.62 $[(M-3Na+H)^{2-}]$, Calcd. for $C_{33}H_{50}N_3O_{22}S_4Na_3$: 1037.15.
14. (a) Davis, N. J.; Flitsch, S. L. *Tetrahedron Lett.* **1993**, *34*, 1181; (b) Anelli, P. L.; Biffi, C.; Montanari, F.; Quici, S. *J. Org. Chem.* **1987**, *52*, 2559.
15. Kovensky, J.; Duchaussoy, P.; Petitou, M.; Sinaÿ, P. *Tetrahedron: Asymmetry* **1996**, *7*, 3119.
16. Spectral data for compound **3**: ^{1}H NMR (600 MHz, D_2O), δ 7.13 (1H, t, J = 8.2 Hz), 7.11 (1H, s), 6.77 (1H, d, J = 8.2 Hz), 6.60 (1H, d, J = 8.2 Hz), 5.44 (1H, d, J = 3.4 Hz), 4.30 (1H, d, J = 7.6 Hz), 4.15 (1H, d, J = 10.3 Hz), 4.01 (1H, d, J = 10.3 Hz), 3.90 (1H, d, J = 11.0 Hz), 3.83–3.82 (1H, m), 3.76–3.71 (3H, m), 3.66–3.60 (6H, m), 3.52 (1H, dd, J = 10.3 Hz, J = 9.6 Hz), 3.42 (3H, s), 3.27–3.18 (3H, m), 3.14 (1H, dd, J = 3.4 Hz, J = 10.3 Hz), 3.07–3.02 (3H, m), 2.34–2.30 (1H, m), 2.30–2.27 (2H, m), 1.88–1.80 (1H, m), 1.65–1.46 (4H, m), 1.35–1.33 (2H, m), ESI-MS (negative mode); Found: *m/z* 484.65 $[(M-3Na+H)^{2-}]$, Calcd. for $C_{33}H_{50}N_3O_{22}S_4Na_3$: 1037.15.
17. Spectral data for compound **4**: ^{1}H NMR (600 MHz, D_2O), δ 7.09 (1H, t, J = 7.9 Hz), 7.04 (1H, s), 6.67 (1H, d, J = 7.9 Hz), 6.52 (1H, d, J = 7.9 Hz), 5.43 (1H, d, J = 4.1 Hz), 4.30 (1H, d, J = 8.2 Hz), 3.91 (1H, d, J = 8.9 Hz), 3.83–3.79 (1H, m), 3.79–3.74 (1H, m), 3.70–3.50 (11H, m), 3.38 (3H, s), 3.25–3.18 (2H, m), 3.14 (1H, dd, J = 9.6 and 9.6Hz), 3.11–2.96 (4H, m), 2.35–2.28 (1H, m), 2.26 (2H, t, J = 6.9 Hz), 1.86–1.80 (1H, m), 1.65–1.45 (4H, m), 1.45–1.27 (2H, m), ESI-MS (negative mode); Found: *m/z* 444.71 $[(M-2Na)^{2-}]$, Calcd. for $C_{33}H_{51}N_3O_{19}S_2Na_2$: 935.21.
18. Binding interactions were measured by use of the SPR imaging sensor, Multi SPRinter (TOYOBO Co. Ltd., Osaka, Japan), under the recommended manufacture's guidelines with slight modification. Array-type Sugar Chips were prepared with the purified ligand-conjugates **1**, **2**, **3**, and **4**. An αGlc-containing ligand-conjugate (Glcα4Glc-mono) was also included in the chips as a non-sulfated control. Typical procedures were as follows. After cleaning the chip surface by UV/O_3 treatment, 1 μl of each sample solution (0.5 mM) in H_2O containing 10% glycerol was spotted on the chip by a spotter (TOYOBO), and left to stand overnight at room temperature. The resulting chip was then washed with water, treated with TEG conjugate[21] to mask the unmodified Au surface, and washed with 0.05% Tween 20 aqueous solution and water in an ultrasonic cleaner. A protein solution in PBS containing 0.05% Tween 20 was injected over the surface at a flow rate of 150 μl/min at various concentrations. The binding interaction was monitored at 25 °C as the change in luminance intensity.
19. Mahalingam, Y.; Gallagher, J. T.; Couchman, J. R. *J. Biol. Chem.* **2007**, *282*, 3221.
20. Cruz, M. A.; Handin, H. I.; Wise, R. J. *J. Biol. Chem.* **1993**, *268*, 21238.
21. TEG conjugate is easily prepared by coupling of thioctic acid and 2-{2-[2-(2-hydroxy-ethoxy)-ethoxy]-ethoxy}-ethylamine.

[Ver: A3B2-WIN8.07r/W-Standard] [25.3.2008–5:40pm] [1–7] [Page No. 1] FIRST PROOFS
{OUP_FPP}jb/mvn038.3d (JBIO)
Paper: mvn038 OUP

J. Biochem. 1–7 (2008)
doi:10.1093/jb/mvn038

One-Step Purification of Lectins from Banana Pulp Using Sugar-Immobilized Gold Nano-Particles

Sachiko Nakamura-Tsuruta[1], Yuko Kishimoto[3], Tomoaki Nishimura[3] and Yasuo Suda[1,2,3,*]

[1]Venture Business Laboratory; [2]Department of Nanostructure and Advanced Materials, Kagoshima University, 1-21-40, Kohrimoto, Kagoshima 890-0065; and [3]SUDx-Biotec Corp., KIBC #461, 5-5-2, Minatojima-minami, Chuo-ku, Kobe 650-0047, Japan

Received December 24, 2007; accepted February 29, 2008; published online March 15, 2008

To obtain lectins without tedious purification steps, we developed a convenient method for a one-step purification of lectins using sugar-immobilized gold nano-particles (SGNPs). Proteins in crude extracts from plant materials were precipitated with 60% ammonium sulphate, and the precipitate was re-dissolved in a small volume of phosphate buffer. The resultant solution was then mixed with appropriate SGNPs under an optimized condition. After incubating overnight at 4°C, lectins in the mixture formed aggregate with SGNPs, which was visually detected and easily sedimented by centrifugation. The aggregate was dissolved by adding inhibitory sugars, which were identical to the non-reducing sugar moieties on the SGNPs. According to SDS–PAGE and MS of thus obtained proteins, it was found that SGNPs isolated lectins with a high purity. For example, a protein isolated from banana using Glcα-GNP (α-glucose-immobilized gold nano-particle) was identified as banana lectin by trypsin-digested peptide-MS finger printing method.

Key words: gold nano particle, lectin, peptide MS fingerprinting, purification, sugar chain.

Abbreviations: CHCA, α-cyano-4-hydroxycinnamic acid; Glcα-GNP, alpha-glucose-immobilized gold nano-particle; GlcNAcα-GNP, alpha-*N*-acetyl-glucosamine-immobilized gold nano-particle; Manα-GNP, alpha-mannose-immobilized gold nano-particle; SA, 3,5-dimethyl-4-hydroxycinnamic acid; SGNPs, sugar-immobilized gold nano-particles.

Lectins are carbohydrate-binding proteins, which can specifically recognize sugar structures (*1*). Their physiological functions have been argued for a long time, and were recently determined for several lectins. Selectins mediate the adhesion of leucocytes and the endothelial cells of blood vessels. Some plant lectins serve as defence factors against phytopathogenic fungi, insect and animals by interacting with their glycans (*2–4*). According to these examples, lectin–glycan interactions are recognized as important in biological processes in both plant and animal bodies. To understand the functions of lectins at the molecular level in detail, purification and subsequent characterization are the most crucial.

To purify lectins from crude extract, several chromatography techniques, such as affinity chromatography, ion-exchange chromatography and gel permeation chromatography, are generally used. However, such chromatographic purification needs lengthy and tedious steps, preventing the studies of lectins especially in case of small amount of target lectins in the starting materials. To overcome this problem, a simple and effective method is desired. Use of gold nano-particles having glycans is one of the most promising for the purpose.

*To whom correspondence should be addressed. Tel.: +81-99-285-8369, Fax: +81-99-285-8369,
E-mail: ysuda@eng.kagoshima-u.ac.jp

Gold nano-particles having glycans were rapidly developed in this decade, and utilized to analyse lectins, to estimate their affinity strength or to visualize them with electron microscopy (*5–7*). Recently, we established an efficient technique for the immobilization of glycans on gold nano-particles (*8, 9*). The produced gold nano-particles, designated sugar-immobilized gold nano-particles (SGNPs), were homogeneous in size and amount of glycans. Importantly, they are easily sedimented by forming aggregate with lectins, suggesting that they are promising for capturing lectins. In this study, we established an effective method for purification of lectins using the SGNPs. As a result, a lectin with high purity was successfully obtained from plant extract.

MATERIALS AND METHODS

Materials—All reagents were used without further purification. Banana was obtained from a grocery store and stored at −20°C until use. Sugars were purchased as follows: maltose, cellobiose and lactose were obtained from Nacalai tesque (Kyoto, Japan); GalNAcβ1-3Gal and α1-2 mannobiose from Dextra Lab. (Reading, UK); melibiose from TCI (Tokyo, Japan). GlcNAcα1-6Glc, GlcNAcβ1-6Glc, GalNAcα1-6Glc, Fucα1-6Glc, Fucβ1-6Glc were generous gifts from Dr Wakao (Kagoshima University).

